MARTIN MARIETTA ENERGY SYSTEMS LIBRARIES
3 4456 0360300 9

CENTRAL RESEARCH LIBRARY
DOCUMENT COLLECTION

ORNL- 113

REACTORS

SA

[redacted]

CLASSIFICATION CHANGED TO: Declassified
BY AUTHORITY OF: TID - 1111
BY: E. Howard 10/22/56

LABORATORY RECORDS
1954

TECHNICAL DIVISION

THERMAL STABILITY OF MULTIPLATE ASSEMBLIES

W.B. ALLRED
G. ASCOLI
H.C. SAVAGE

OAK RIDGE NATIONAL LABORATORY
CENTRAL RESEARCH LIBRARY
CIRCULATION SECTION
4500N ROOM 175
LIBRARY LOAN COPY
DO NOT TRANSFER TO ANOTHER PERSON
If you wish someone else to see this report, send in name with report and the library will arrange a loan.
UCN-7969 (3 9-77)

[redacted]

OAK RIDGE NATIONAL LABORATORY

DIVISION OF
CARBIDE AND CARBON CHEMICALS CORPORATION
POST OFFICE BOX P
OAK RIDGE, TENNESSEE

[redacted]

[redacted]

ORNL-113

This document consists 52 pages.

Contract No. W-7405 - Eng. 26

Copy 5 of 83 Series A.

OAK RIDGE NATIONAL LABORATORY

ISSUED: 706 - B. Library

Technical Division

Section II

C. E. Winters - Section Chief

****

Final Report

Problem Assignment No. TX12-5

THERMAL STABILITY OF MULTIPLATE ASSEMBLIES

W. B. Allred
G. Ascoli
H. C. Savage

July, 1948

Date Received: 8/5/48 Date Issued: AUG 25 1948

[redacted]

[redacted]

MARTIN MARIETTA ENERGY SYSTEMS LIBRARIES

3 4456 0360300 9

TABLE OF CONTENTS

1.0	ABSTRACT	3
2.0	INTRODUCTION	4
3.0	NORMAL TEMPERATURE PATTERNS	6
4.0	ABNORMAL TEMPERATURE PATTERNS	13
5.0	THERMAL STRESS ANALYSIS	15
6.0	DESCRIPTION OF APPARATUS	25
7.0	EXPERIMENTAL RESULTS	28
8.0	ESTIMATION OF ERROR	41
9.0	APPENDIX	42
9.1	DERIVATION OF EQUATION DEFINING TEMPERATURE DISTRIBUTION IN A URANIUM ASSEMBLY BASED ON NEUTRON FLUX PATTERN	42
9.2	DERIVATION OF EDGE EFFECT EQUATIONS	43
9.3	DERIVATION OF EQUATIONS OF TEMPERATURE GRADIENT THROUGH THICKNESS OF ASSEMBLY PLATES	49
9.4	DERIVATION OF EQUATION OF ABNORMAL CHANNEL WIDTH ON PLATE TEMPERATURE	50

[redacted]

1.0 ABSTRACT

This report covers in some detail the problem of thermal stability of the uranium fuel assemblies when subjected to operating temperature conditions expected in the High Flux Research Pile. The investigation of the problem includes a study of multiplate assemblies containing 1.5 m.m. thick plates with 0.0203 grams 25/cm^2 and having a 3 m.m. annular spacing, and of assemblies containing 1 m.m. thick plates with 0.0142 grams 25/cm^2 and having a 2 m.m. annular spacing. Experimental results reported here deal only with all aluminum assemblies.

The following results and conclusions are reported for a representative aluminum assembly containing 18 curved plates 60 cm long, 7.61 cm wide, and 0.15 cm thick:

1. An analysis of thermal stresses reveals that no serious stresses exist in a multiplate assembly. Maximum tensile stress is 2800 psi and maximum compressive stress is 1700 psi; whereas a stress of approximately 4000 psi is required to distort the assembly permanently.
2. Experimental results show a maximum bowing of the fuel plates of 0.005 inches or less. Calculated stresses in the plate can result in deflections of this magnitude.
3. Longitudinal expansion of the fuel plates for a temperature change from 20° C to the elevated temperature pattern in the pile is a maximum of 0.025 inches. Calculated expansion of the 60 cm long plate is 0.022 inches.

[redacted]

4. Expansion of the assembly in a lateral direction is less than 0.002 inches.

5. A maximum change in plate temperature of 20° F is calculated for the case of a decreased annular spacing of 50%.

Temperature patterns which may be expected in the uranium plate assemblies under pile operating conditions were calculated and are submitted along with experimentally obtained patterns.

2.0 INTRODUCTION

An investigation was conducted on the uranium fuel assemblies to be used in the proposed High Flux Pile to determine their thermal stability under pile operating temperature conditions. The scope of the investigation covered a theoretical study of normal and some abnormal temperature patterns in the assemblies at pile operating heat levels; the determination of resulting thermal stresses, thermal expansion, and thermal buckling; and the reproduction of the thermal conditions and their effects in experimental assemblies of the following two types:

(a) Multiplate assemblies containing parallel, 1 m.m. thick, aluminum plates with a 2 m.m. annular spacing.

(b) Multiplate assemblies containing parallel, 1.5 m.m. thick, aluminum plates with a 3 m.m. annular spacing. It is planned to use this type of assembly in the High Flux Pile.

Design specifications used as a basis for theoretical and experimental work for the two cases are:

	1 m.m. Plates(1)	1.5 m.m. Plates(2)
Maximum power level in pile	30,000 KW	30,000 KW
Neutron flux distribution	$f(n) = \cos \pi x/78$	$f(n) = \cos \pi x/78$
Weight of 25 in pile	3500 grams	3500 grams
Concentration of 25 in sandwich	0.0142 gms/cm^2	0.0203 gms/cm^2
Unit heat production	142 watts/cm^2	203 watts/cm^2
Active length of plates	60 centimeters	60 centimeters
Cooling water flow rate	30 feet/second	30 feet/second
Inlet temperature of cooling water	80° F	100° F
Heat transfer coefficient	3700 Btu/(hr)(ft^2)(°F)	5175 Btu/(hr)(ft^2)(°F)
Thickness of flat aluminum sheet	1.0 millimeter	1.5 millimeter
Water Gap	2.0 millimeter	3.0 millimeter

A theoretical study was made for both of the parallel plate assemblies; however the testing program dealt primarily with the 1.5 m.m. multiplate assembly. Preliminary tests were conducted on a single 1 m.m. flat plate and on 1 single 1.5 m.m. flat and curved plates. Experimental assemblies were fabricated of 2 S-0 aluminum.

---

1. Leverett, M. C. and Huffman, J. R., "Technical Division Preliminary Process Design Report 1000 Project," Clinton Laboratory, May 15, 1946.

2. Huffman, J. R., "Heterogeneous Pile - 1000 Project - Design Data Sheets," Clinton Laboratory, May 14, 1947.

3.0 NORMAL TEMPERATURE PATTERNS

Examination of the temperature distribution in the uranium fuel assemblies under pile operating conditions may be divided into three parts:

(a) Temperature distribution which results from the neutron flux pattern in the assembly.

(b) Temperature gradient which occurs along the edges of an active sandwich plate which is caused by heat conducted from the heat producing sandwich to the non-heat producing aluminum sealing strip.

(c) Abnormal temperature conditions.

The neutron flux pattern in the 60 cm long uranium assemblies is defined as:

$$f(n) = \frac{\cos \pi x}{L}$$

where x is the distance in centimeters along the length of the assembly from its center, and L is the effective length of the assembly which is 78 centimeters, or 60 centimeters plus an added length of 9 cm at each end required by the reflector. This equation is modified to define the longitudinal temperature distribution in a 60 centimeter long assembly as follows:(3)

$$(1) \quad Tx = (A/hp) \cos \frac{\pi x}{L} + \frac{AL}{CW\pi} \left(\sin \frac{\pi x}{L} + \sin \frac{\pi b}{L}\right) + Tw$$

Tx = plate surface temperature at any point x - °F

Tw = inlet water temperature - °F

A = a constant defined as $Q = A \int_{-b}^{b} \cos \pi X/L \, dx$; Btu/(hr)(ft)

---

3. Derivation of the equation is presented in Appendix 9.1.

h = heat transfer coefficient - Btu/(hr)(ft^2)(°F)

p = perimeter of heat transfer surface - ft.

C = heat capacity of water - Btu/(lb)(°F)

x = longitudinal distance from center of assembly - feet

b = length of assembly from its center - feet

W = weight flow of cooling water - lbs/hr

L = effective length of assembly - feet

The distribution takes the form of a skewed cosine curve. Temperature plots for each set of design specifications are presented in Figure 1.

The temperature gradient which occurs along the edges of the active plates in the area of the interface between the uranium-aluminum sandwich and the aluminum sealing strip is considered. Heat is generated in the sandwich but not in the sealing strip; thus heat flows between the two areas. See Figure 2. The problem is hardly this simple, however, since heat is also lost at the plate surfaces. The case of a plate infinitely wide in two directions from an interface is considered as the simplest case. The enriched uranium sandwich is in one direction and the aluminum sealing strip is in the other. Then, consider that heat is either transferred along the axis of the plate or lost at the plate surfaces. From these considerations the following equations may be derived to determine the surface temperatures along the sandwich edge.[4]

---

4. Derivation of equations is presented in Appendix 9.2.

[redacted]

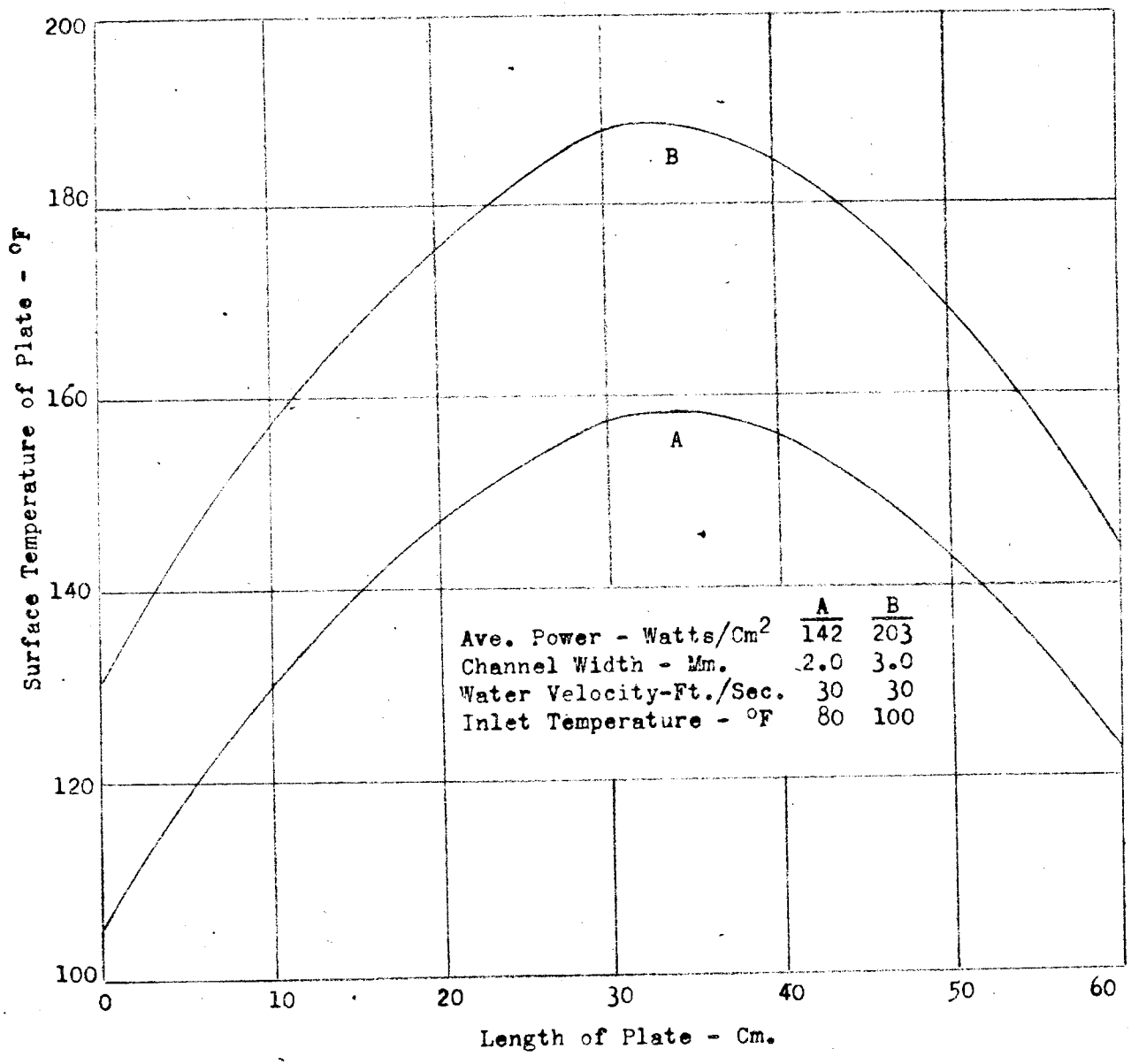

FIGURE 1 CALCULATED LONGITUDINAL TEMPERATURE DISTRIBUTION ALONG PLATE CENTER LINE IN THE DIRECTION OF WATER FLOW

[redacted]

Drawing # 5955

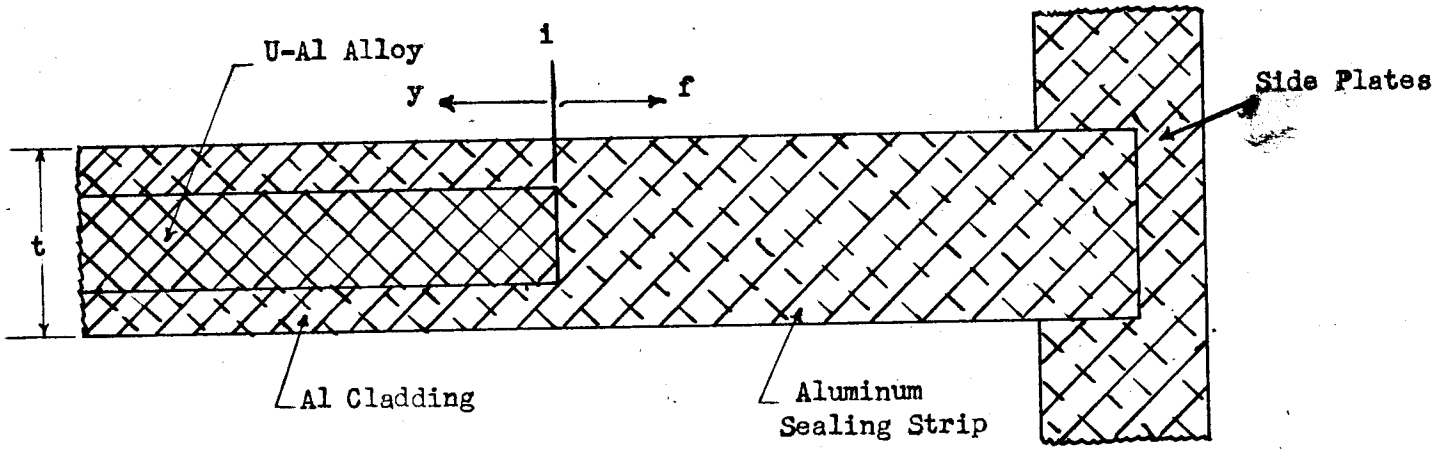

FIGURE 2 - CROSS SECTION OF ACTIVE PLATE EDGE

Not to Scale

Drawing # 5956

(2) $T_y = T_m - T_i\, e^{-\sqrt{\frac{tk}{2h}}\, y}$ for the enriched sandwich

(3) $T_f = T_i\, e^{-\sqrt{\frac{tk}{2h}}\, f}$ for the aluminum sealing strip

where:

T_y, T_f = surface temperature above water temperature - °F

T_m = maximum surface temperature above water temperature - °F

t = thickness of plate - ft

k = metal thermal conductivity coefficient - Btu/(hr)(ft^2)(°F)/ft

h = water film coefficient on metal surface - Btu/(hr)(ft^2)(°F)

y = distance from interface on the enriched uranium sandwich - ft

f = distance from interface on the "dead" aluminum strip - ft.

T_i = surface temperature above water temperature at the interface - °F

It is necessary to justify the use of the equations for an infinitely wide fin when the case being considered is for a fin of finite length. The justification arises from the thinness of the fin. Heat flow from the fin surface is far greater than the heat flow along the fin axis. It is expected, therefore, that the heat flux and fin temperature will reach a plateau within a short distance in the y direction from the interface. Conversely, in the f direction from the interface the heat is dissipated within a short distance. Therefore, the end conditions in each direction from the interface of the finite fin approximate those of the fin cross section at an infinite distance.

Calculated values obtained from equation (1) show that a maximum surface temperature of 190° F exists in the 1.5 m.m. thick active plates and 162° F in the 1 m.m. plates. Respective temperature drops at the plate edges in these cases calculated from equations (2) and (3) are 76° F and 52° F. Theoretically determined curves for each case are presented in Figure 3.

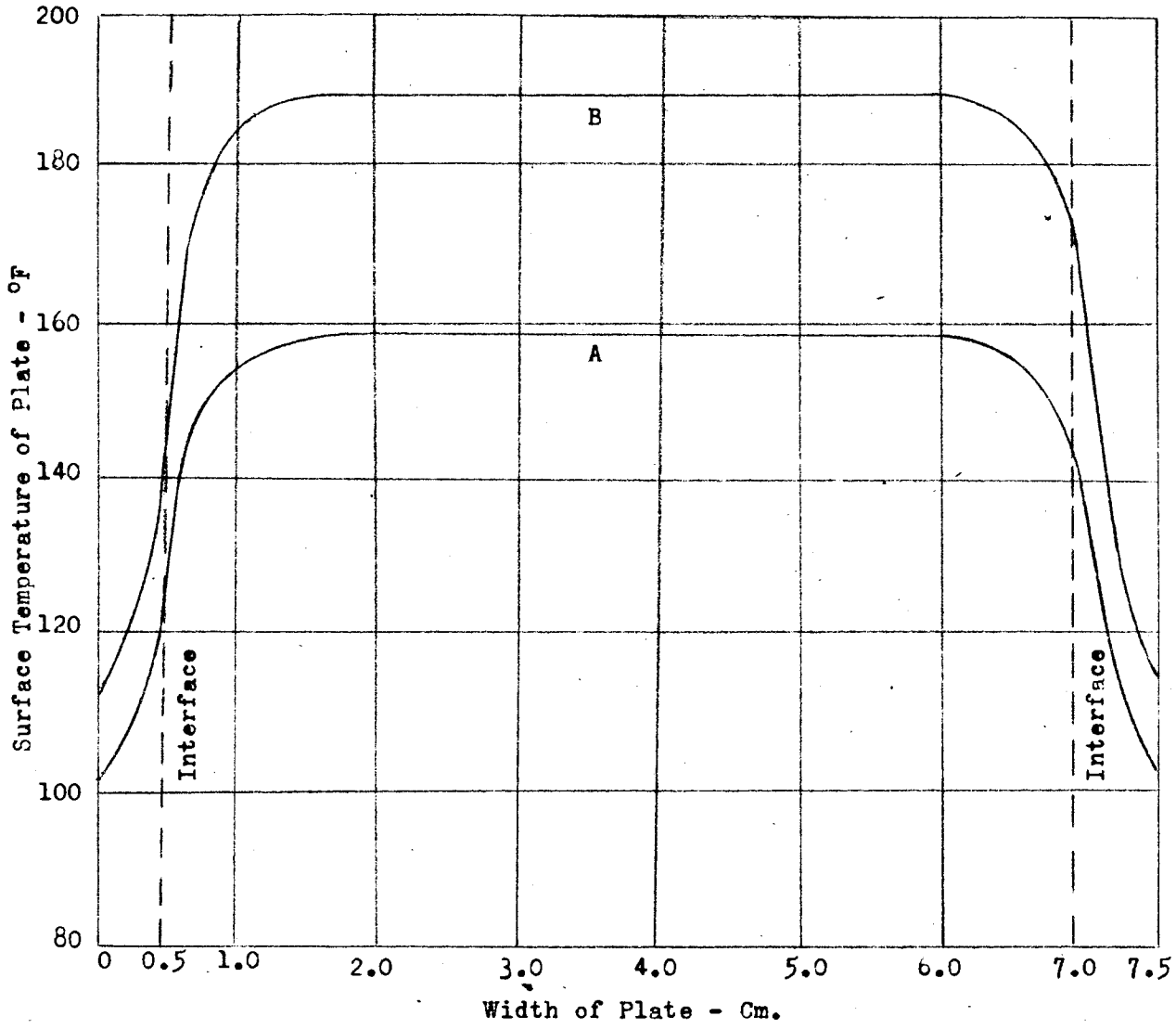

FIGURE 3 LATERAL TEMPERATURE DISTRIBUTION SHOWING DROP AT INACTIVE EDGES

	A	B
Ave. Power - Watts/Cm^2	142	203
Channel Width - Mm.	2.0	3.0
Water Velocity - Ft./Sec.	30	30
Inlet Temperature - °F	80	100

Drawing # 5957

When the side plate thickness was increased in the assembly design, it was recognized that the geometry of the sealing edge could no longer be considered a fin. In earlier work one fifth of the plate sealing edge was a part of the side plate, and a major part of the heat loss occurred in the finned section. In the current design four fifths of the edge is an integral part of the side plate, and the side plate contribution to cooling is of more importance. Therefore, the heat flux pattern cannot be treated as in the case of a fin. A graphical method(5) was used to determine the patterns of heat transfer in the new geometrical shape which resembles a "T".

Further refinement of the equations (2) and (3) was made to include the effect of hot spots at the assembly active plate edges. The slowing down effect of water on fast neutrons and the relationship of heat flux to slow neutron flux are well known. Since the water/25 ratio is greater at the assembly edges than at the center, a higher heat flux and a resulting local hot spot exist. A similar condition exists in assemblies adjacent to the beryllium reflector because of a higher slow neutron level occurring there. The extreme case of edge flux/minimum flux for a plane normal to the major axis of an assembly, as determined by Spinrad(6), using two group theory, exists between the normal

---

5. McAdams, W. H., Heat Transfer, 2nd edition. McGraw Hill 1942, Page 16. A Solution of the problem is presented in Appendix 9.2.

6. Spinrad "Assembly Edge Hot Spots", May 25, 1947. The procedure is presented in Appendix 9.2.

25 and control 25 assemblies and is 1.22. The hot spot effect was taken as starting 3 centimeters from the assembly edge, and a plot of the flux pattern was made. By graphical integration a corrected quantity of heat flowing along the plate axis was calculated to be 1.095 Q, where Q is the uncorrected value of heat flow.

An extreme case of 1.20 Q was also calculated for comparison.

The temperature gradient across the active plate edges and side plates for the 3 cases of heat flow are plotted in Figure 4.

4.0 ABNORMAL TEMPERATURE PATTERNS

The previous section discussed the temperature distribution in a balanced or normal system where heat production and removal are the same in adjacent elements. Several factors may cause a departure from this ideal state, for instance: changes in flux near a control rod, irregualr spacing of assembly plates, and variations in fuel concentration within the assemblies. Furthermore, if the symmetry of the assemblies is destroyed, temperature differences between faces of the same plate will be established. Only those temperature differences which take place over a very short distance are of concern; therefore the following paragraphs present situations in which temperature differences between adjacent plates exist.

4.1 Temperature Gradient Through the Thickness of a Plate

When heat is removed at different rates from opposite faces of an assembly plate there results a linear temperature variation across the plate superimposed

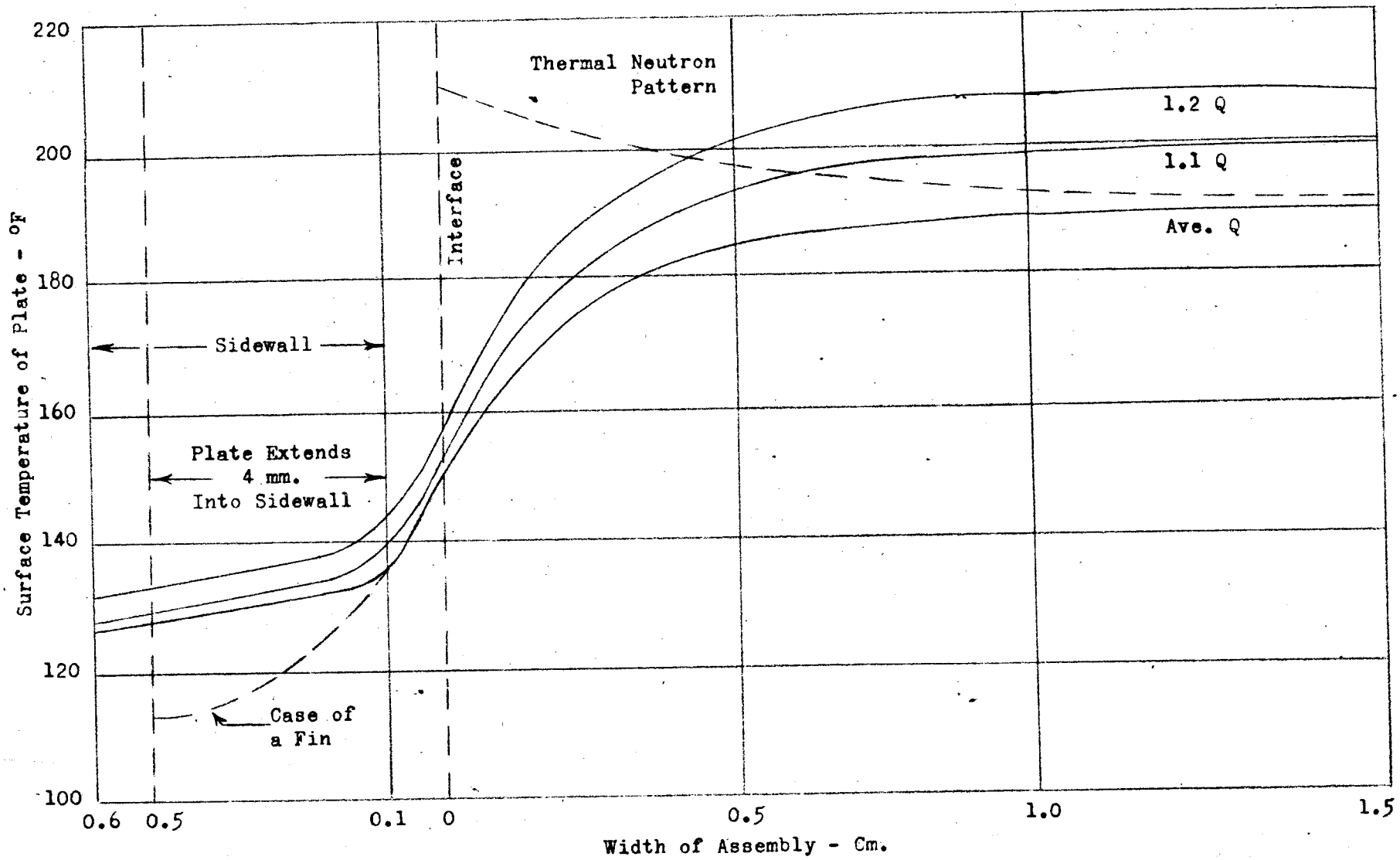

FIGURE 4 CALCULATED TEMPERATURE DROP AT PLATE EDGES SHOWING HOT SPOT EFFECT OF THERMAL NEUTRONS
(Case of 6 mm. Inactive Edge - 1 mm. Fin Plus 5 mm. Sidewall)
(Case of 1.5 mm. thick Fuel Plate With a Unit Heat Production of 203 watts/cm^2)

Drawing # 5958

on the usual symmetrical distribution. Such a condition is established when the annular spaces on each side of the plate have unequal thickness. The case is illustrated in Figure 5.

A derivation of equations for t_1 and t_2 is presented in Appendix 9.3. Temperature difference between opposite faces of a plate is plotted as a function of the ratio of abnormal to normal annular width in Figure 7.

4.2 Abnormal Channel Width

If the width of a channel differs from that of its neighbors, the changed rate of flow of the coolant results in different water and plate temperatures. The case is illustrated in Figure 6.

From the sketch, channel a-a' is smaller than adjacent channels. Since less coolant flows in this channel, plates a and a' are hotter than adjacent plates. A plot of maximum deviation from normal plate temperature vs effect of abnormal channel width is presented in Figure 7. A derivation of equations defining this effect is presented in Appendix 9.4.

5.0 THERMAL STRESS ANALYSIS

The temperature patterns peculiar to the uranium fuel assemblies will produce thermal stresses in a number of places. In assemblies of proper dimensions, of uniform 25 content, and under normal operating conditions, the most serious stress occurs near the sandwich edge at the interface between the enriched uranium sandwich and the aluminum sealing edge. See Figure 3. Since

[redacted]

Drawing # 595

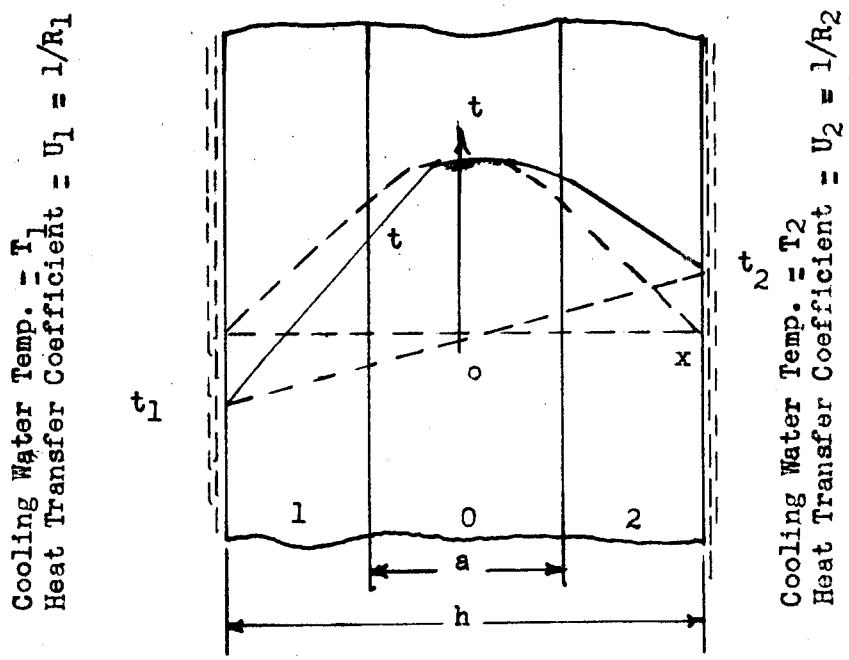

FIGURE 5 - TEMPERATURE GRADIENT THROUGH THICKNESS OF PLATE

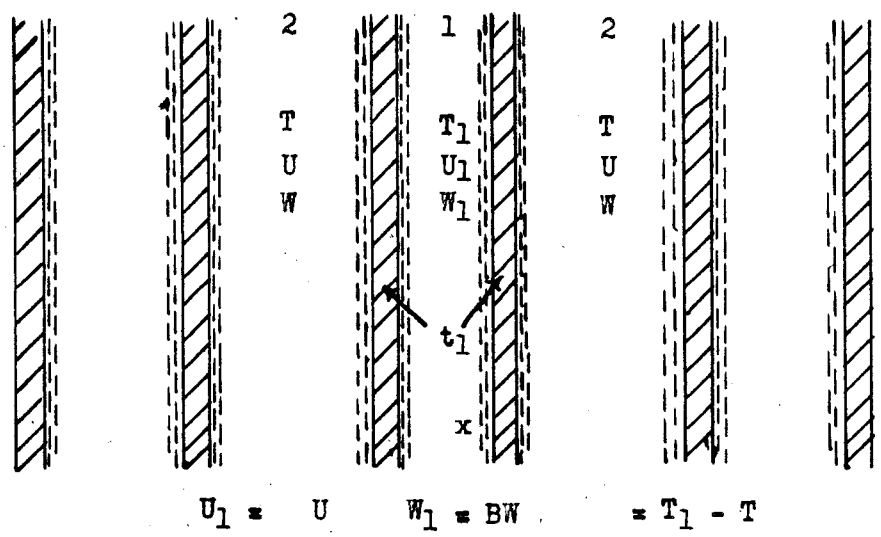

FIGURE 6 - ABNORMAL CHANNEL WIDTH

[redacted]

[redacted]

Drawing # 5960

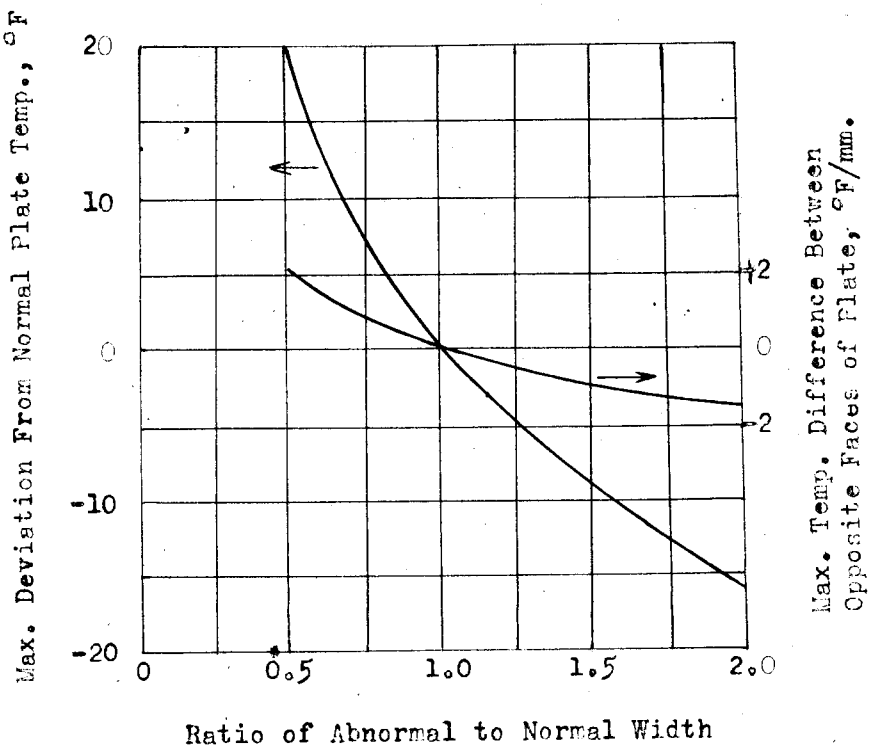

FIGURE 7 - EFFECT OF ABNORMAL CHANNEL WIDTH ON PLATE TEMPERATURE

[redacted]

the temperature gradient per unit distance in this area is the maximum in the assemblies the resulting stress is the maximum.

Consider the case of an area with a temperature gradient in the x direction and a constant temperature in the y direction.

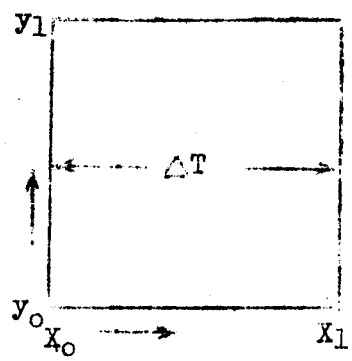

Figure 8

The ΔT from x_o to x_1 sets up a strain which is calculated as follows:

$$\sigma y = \alpha L \Delta T$$

where α = coefficient of thermal expansion

L = unit length of area in y direction.

Tensile stress is calculated as:

$$S_s = \frac{\sigma s \quad E}{(1 - \nu)}$$

where E = Modulus of Elasticity

ν = Poissons ratio

Stress at the sandwich interface can be treated by another method. A temperature drop occurs across the 1.5 c.m. edges under pile operating conditions which results in a difference in longitudinal expansion of the active plate edge and of a plane 1.5 c.m. from the plate edge. It is apparent that the colder edge of the plate has the effect of restraining expansion of hotter portions. A compressive force can be calculated which if applied at the longitudinal ends of the plates will restrict expansion in a like manner.

Calculated results obtained from these two methods are submitted for comparison in Table 1 for the case of a 1 m.m. thick plate assembly and of a 1.5 m.m. thick plate assembly with both 4 and 5 m.m. thick side plates.

From the table it is noted that normal maximum stress which occurs in any one of the design cases considered is less than 4000 psi; whereas a stress of 5000 psi is required to permanently distort the assembly plates. Although the results obtained by the two methods are not in close agreement, they are of the same order of magnitude and are not large enough to be considered serious.

Stress of the order of 1/50 of the edge effect stress results from the longitudinal cosine temperature pattern. This stress is considered insignificant.

It can be expected that abnormal variations of the assembly temperature patterns will set up some stresses. A study of those stresses was made for cases covered in section 4.0. The case of a channel restricted by 50% with

a resulting temperature rise in the affected plates of 20° F is considered. The calculated case indicated a difference in expansion of the plates of less than 0.001 inches. Curved active plates would increase in curvature to relieve the strain. It is difficult to visualize significant stresses set up in such a case. Experimental results of such a case reported in a later section bear out this conclusion.

Another condition of a temperature gradient over a short distance occurs between faces of the same plate. Calculated stresses for this case are of the order of 500 psi and are not considered serious.

Thermal stress calculations were made using mechanical constants for 2S-0 aluminum rather than for U-Al alloy since small error results and since experimental models were aluminum. All stresses are reduced by 1.5% when the coefficient of thermal expansion for 22% uranium in aluminum by weight is used and by 3% for 30.5% uranium in aluminum by weight. In view of the insignificance of the correction only the percentage values are presented. A thermal conductivity correction increases surface temperatures by 10% for the 22.7% uranium-aluminum alloy; however, the temperature gradients causing thermal stress do not change appreciably.

TABLE 1

THERMAL STRESSES AND EXPANSION

	Multiplate Assembly 1 mm thick plates	Multiplate Assembly 1.5 mm thick plates	
		5 mm Side plates	4 mm Side plates
1. Maximum - ΔT °F/mm.	20	15	15
2. Maximum Calc. edge effect Tensile Stress - PSI	3800	2810	2810
3. Maximum Calc. edge effect Compression Stress - PSI	1600	1720	1300
4. Maximum Calc. Longitudinal Expansion - Inches	0.022	0.021	0.022
5. Maximum Exp. Longitudinal Expansion - Inches	-	-	0.025-0.030
6. Maximum Calc. Lateral Expansion - Inches	-	.002	0.002
7. Maximum Exp. Lateral Expansion - Inches	-	-	0
8. Maximum Calc. Long Bowing - Inches	0.005	-	0.005
9. Maximum Exp. Long Bowing - Inches	0.005	-	0.005
10. Maximum Calc. Longitudinal Tensile Cosine Temperature Gradient - PSI	46	57	57
11. Tensile from ΔT between plate faces - PSI	390	390	390

5.1 Abnormal Stress Conditions

The bonds between the uranium-aluminum alloy sheets and the cladding aluminum sheets will be checked by X-ray photographs and by bend tests. In addition any poor bond usually results in a blister during the brazing operation. However, it is possible that perfect bonds would not be formed in all cases during the rolling operations and might not be detected on inspection.

We may consider two assumed cases of lack of complete bonding. These are, first, no bonds along the edges or ends of the uranium-aluminum alloy sheets and for a distance of one milimeter (assumed as one diameter) back on each side and, second, small areas on one side of the plate.

The case of poor edge bonding is illustrated in Figure 8A. This figure shows the heat flow pattern estimated for this condition. No attempt has been made to analyze this problem completely from a theoretical study but rather the graphical solution method described by McAdams(7) has been used. The average uranium-aluminum alloy temperature may be estimated as 205° F by use of the data presented in paragraph 4.3 of report MonT-433(8). From

---

7. McAdams, W. H., "Heat Transmission," McGraw-Hill Book Co., New York, second edition, 1942, page 16.

8. Huffman, J. R., Leverett, M. C., Newson, H. W., and Weinberg, A. M., "Feasibility Report on Clinton High Flux Pile," December 1, 1947

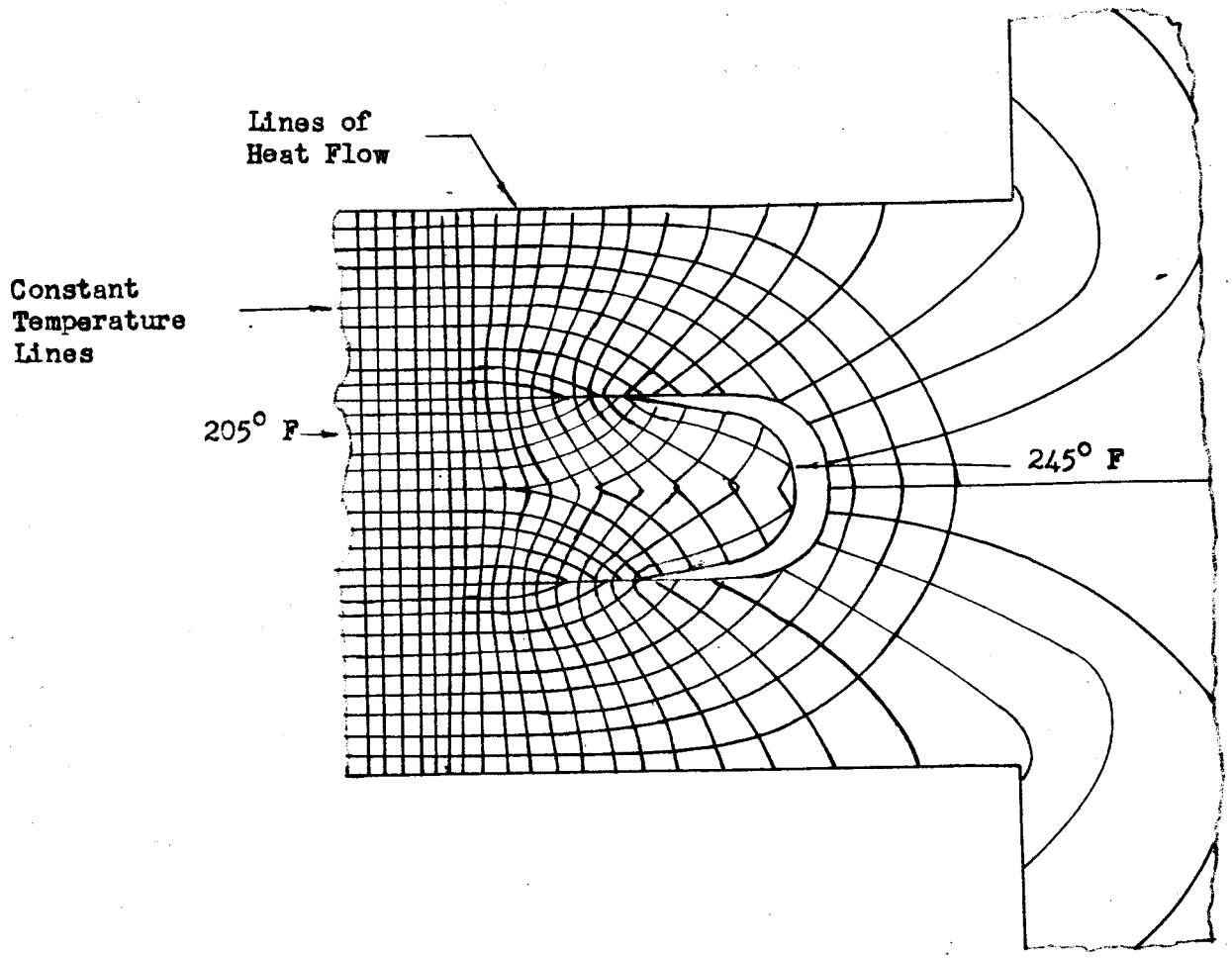

FIGURE 8A - HEAT FLOW AT POORLY BONDED EDGE

Drawing # 5961

this and Figure 8A, the maximum temperature at the center of the edge of the poorly bonded section is estimated as 245° F. While this method is not too accurate, the actual maximum temperature probably would not be more than 5° F from this value.

In the second case in which we may have poorly bonded areas on the sides of the plates the heat flow would be unidirectional away from the poor bond with the exception of the heat flow across the poor bond or free space. In this case excessive temperatures would not occur as the average water temperature would be increased at most from 107° F to 121° F and the average alloy temperature from 205° F to 303° F.

The question may be asked regarding the shear produced by the temperature differences in the uranium-aluminum alloy and in the adjacent poorly bonded aluminum sheet. Assuming an alloy plate temperature of 303° F (no restraint due to pure Al sheets is assumed) and an aluminum plate temperature of 107° F, the shear in the aluminum per square inch for a poorly bonded area one inch in diameter may be calculated as follows:

$$\text{Increase in length per inch} = (303-107)\,\frac{.224 \times 10^{-4}}{1.8} = .00254$$

$$\text{Shear force} = .00254 \times 10^{7} \times 1 \Big/ 1 = 25{,}400 \text{ psi.}$$

While this stress is above the yield point, it cannot cause failure since aluminum is a ductile material. Any high stress will simply stretch it beyond the yield point without great increase in stress.(9)

---

9. Timoshenko, S., "Strength of Materials," Part II., D. Van Nostrand Co., New York, 1941, page 323.

5.2 Diffusion of Fission Products

Results of tests and theoretical calculations reported in MonT-342[10] show that the diffusion of fission products through aluminum is negligible.

6.0 DESCRIPTION OF APPARATUS

Apparatus used in experimentally determining thermal stability of the fuel assemblies was required to satisfy the following conditions:

1. Reproduce and measure the temperature patterns which are expected in an assembly under pile operating conditions.
2. Measure thermal expansion and warping resulting from the imposed temperature conditions.

The description presented here deals only with multiplate assembly testing apparatus. Techniques of heating, cooling, and warping measurement are similar for the single plate experiments.

The most serious temperature gradient over a short distance in the assemblies results from the edge effect. Therefore, heating and cooling methods used were primarily to produce this effect.

Heating was supplied to the active plates from mica-jacketed chromel resistance heaters inserted longitudinally in each annulus and placed about one and one half centimeters from the side plates, thus maximum heat to the

10. "The Diffusion of Fission Products in Aluminum," by G. Ascoli, July 14, 1947

active plates was applied at the edges in the region where heat removal was a maximum. See Figure 9. The temperature plateau, Figure 3, is obtained by heat flow along the plate to the center. Heat losses to the ambient air were sufficient to maintain an approximate plateau effect. The sharp drop at the edges was accomplished by the rapid removal of heat through the assembly side plates.

Heat removal was accomplished by spraying water on the side plates. The water was ejected through small holes drilled in a pipe header which was mounted such that the water spray struck the top of the side plates; blanketed the plate surface, thus supplying the needed cooling action; and was caught in a withdrawal pan underneath.

The cooling water was supplied in sufficient volume to produce a nearly constant side wall temperature.

Temperature measurements were accomplished by two methods. A number of thermocouples were brazed during assembly fabrication on 5 of the 18 "active" plates at points only along the lateral center plane at several points down the length. Since the thermocouple leads were placed in the annular spacing between plates, it was necessary to limit the number of couples to allow installation of strip heaters in each annulus. To supplement the attached thermocouples a surface contact thermocouple was used to make temperature measurements at other points. The contact couple was made by inserting a

[redacted]

Drawing # 5962

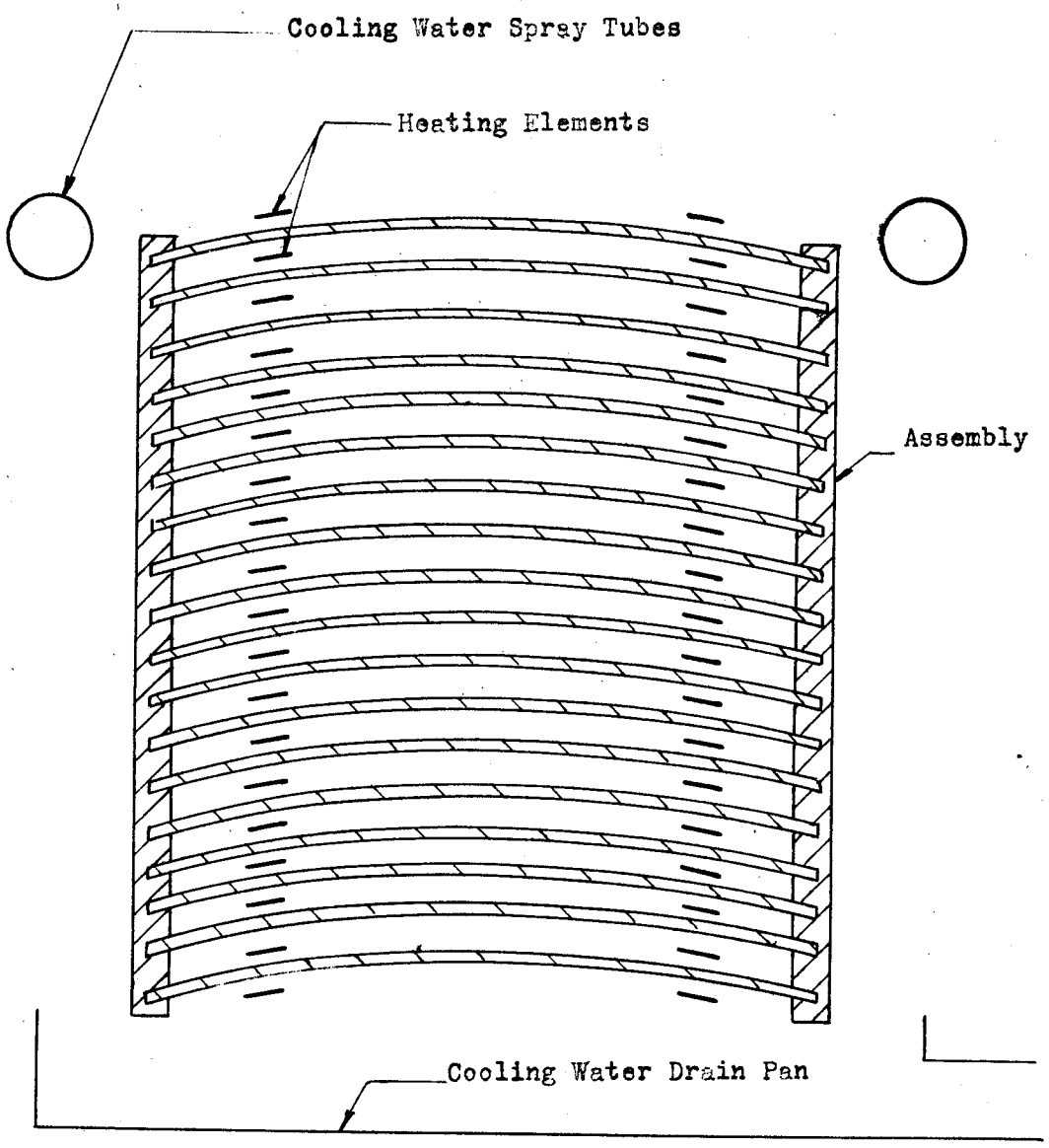

FIGURE 9 - CROSS SECTIONAL VIEW OF MULTIPLATE ASSEMBLY TEST APPARATUS

[redacted]

#30 alumel wire into a hypodermic needle and insulating the two except at the hot junction. Small holes were drilled to several plates to allow contact measurements to be taken.

Test assemblies were mounted in a water cooled reference stand in such a manner that displacement was improbable but expansion was not restricted. The reference stand was maintained at a constant temperature to eliminate possible dimensional changes from temperature variation. During a number of heating and cooling cycles of the assemblies, reference dimensions on the stand remained constant within the accuracy of measurement (0.0005"). Therefore, changes in distance from the reference stand to the assembly were considered to be buckling of the plates. Buckling of the plates was measured with a depth micrometer.

A cathetometer mounted over the test assemblies was used to determine the amount of longitudinal expansion and lateral bowing during the heating and cooling cycles. See Figure 10.

7.0 EXPERIMENTAL RESULTS

Temperature patterns calculated to produce significant thermal stresses in the enriched uranium fuel assemblies were reproduced in experimental assemblies. Temperature levels for both sets of design specifications were obtained, namely: (a) Plates producing 203 watts/cm^2 (b) Plates producing 142 watts/cm^2. The "edge effect" temperature gradient was accomplished in

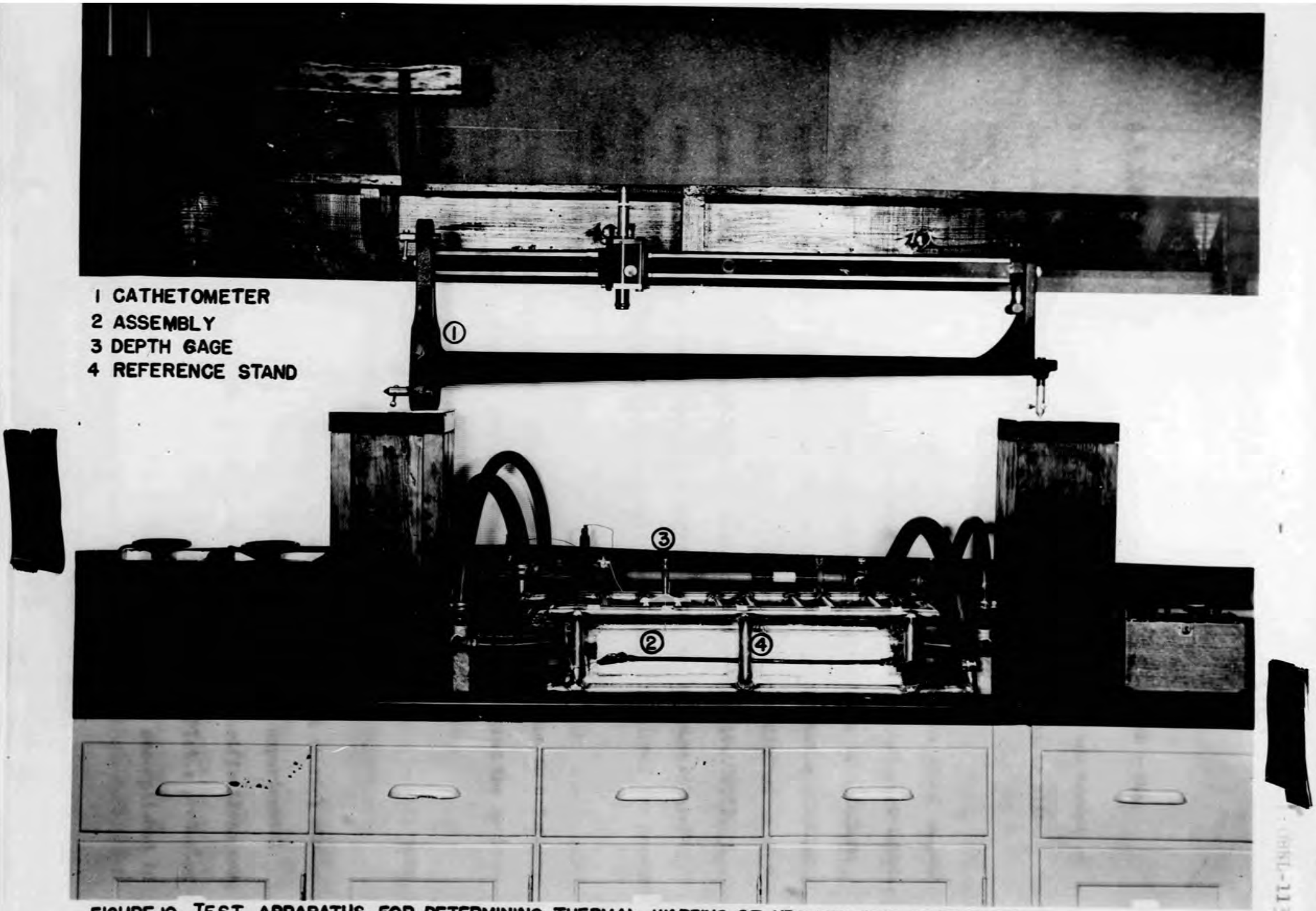

FIGURE 10 TEST APPARATUS FOR DETERMINING THERMAL WARPING OF URANIUM FUEL ASSEMBLIES

single plate and multiplate test models, and its effects were thoroughly investigated since it produced the most serious stresses. See Figures 11 and 12. The less important cosine temperature curve, from the standpoint of the stress investigation, was produced only in single plate models. See Figures 13 and 14. The small temperature drop of 0.2 ^{o}C/mm produced insignificant thermal stress. Since the heating techniques involved to accomplish the cosine distribution were extremely tedious, it was not considered worthwhile to further complicate the heating circuits. Furthermore, experimental deflection results from single plate models in which the cosine temperature curve was produced agreed remarkably well with results from multiplate assemblies where no cosine distribution was attempted.

The maximum deflection in the 1.5 mm active plates in the curved multiplate assemblies was 0.005 inches when normal temperature patterns expected in the pile were produced. Deflection of the plates took the form of a longitudinal bowing. Deflection was a maximum at the longitudinal and lateral center of the active plates and a minimum at the longitudinal ends. A net bow of the order of 0.005 inches was observed in a statistically significant number of tests. The arch of the bowing was in the direction of the plate curvature. Deflection at the plate center was, therefore, in the direction of designed curvature, however, the plate ends in some cases deflected in the opposite direction. See Figure 15. The condition is not unexpected when the stress patterns there are known. The magnitude of deflection at the plate ends was $\pm$ 0.001 - 0.002 inches. Plate deflection

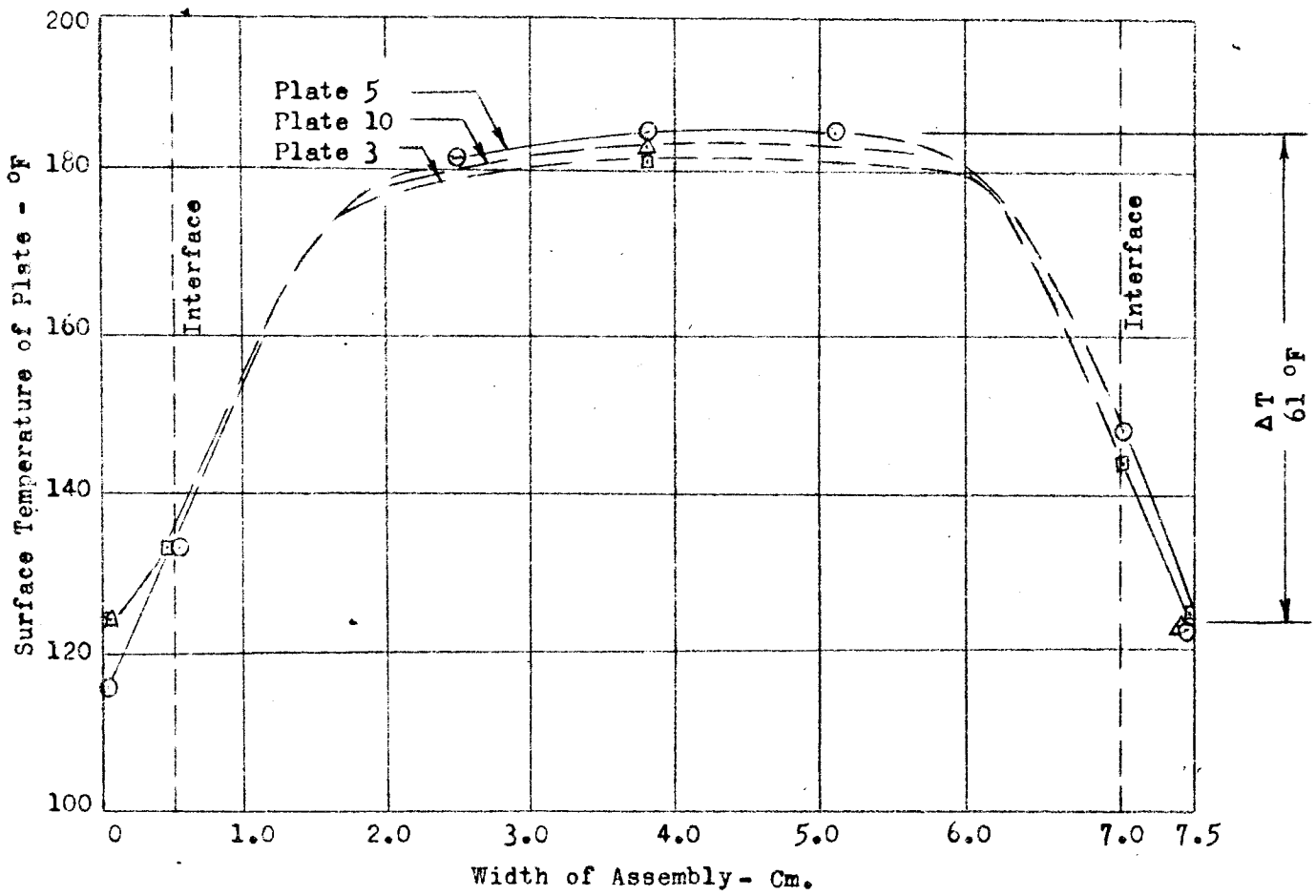

FIGURE 11 LATERAL TEMPERATURE DISTRIBUTION PRODUCED EXPERIMENTALLY IN A MULTIPLATE ASSEMBLY CONTAINING 18 CURVED PLATES

[redacted]

Drawing # 5963

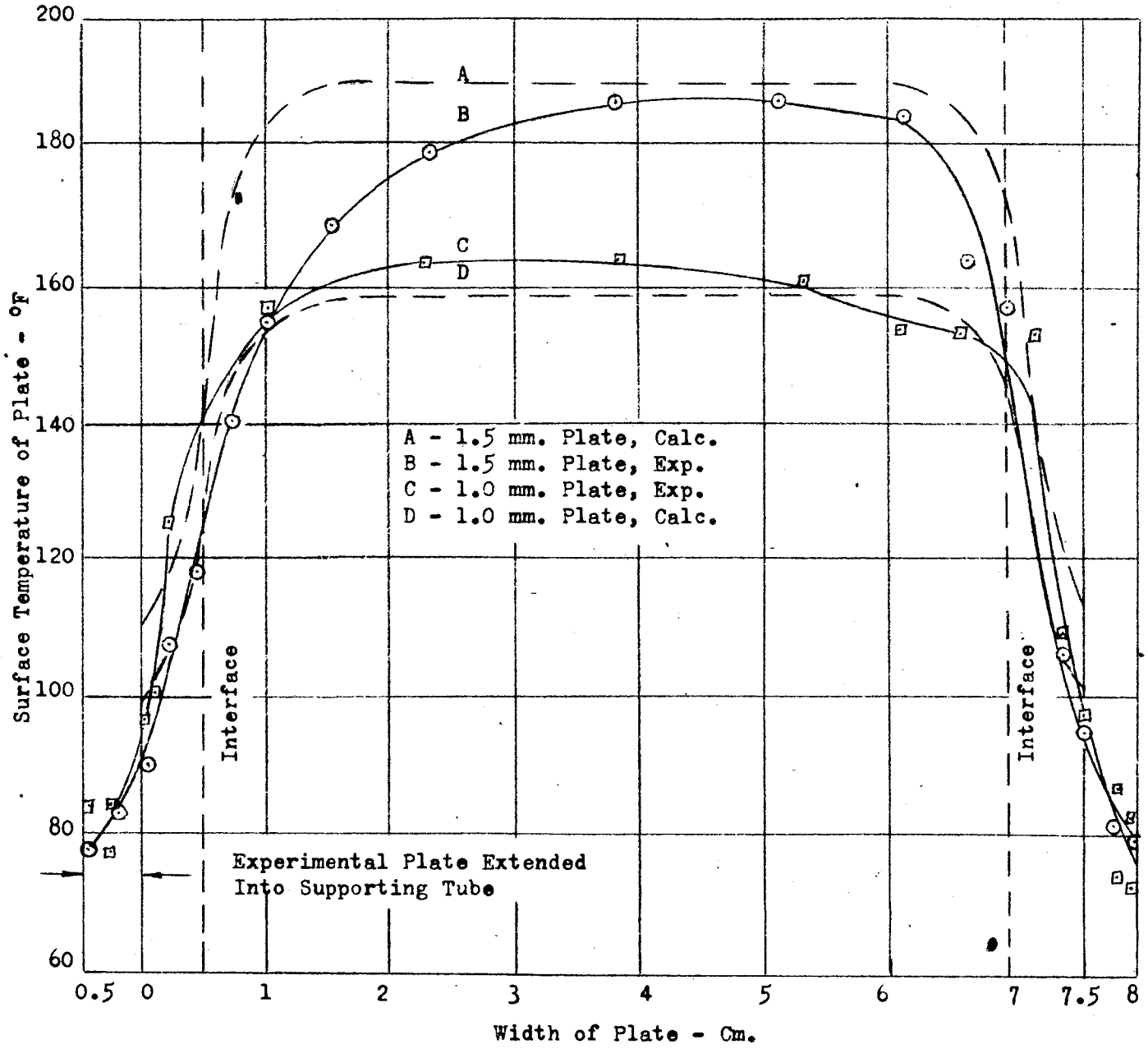

FIGURE 12 LATERAL TEMPERATURE DISTRIBUTION PRODUCED EXPERIMENTALLY IN SINGLE PLATE ASSEMBLIES

Drawing # 5964

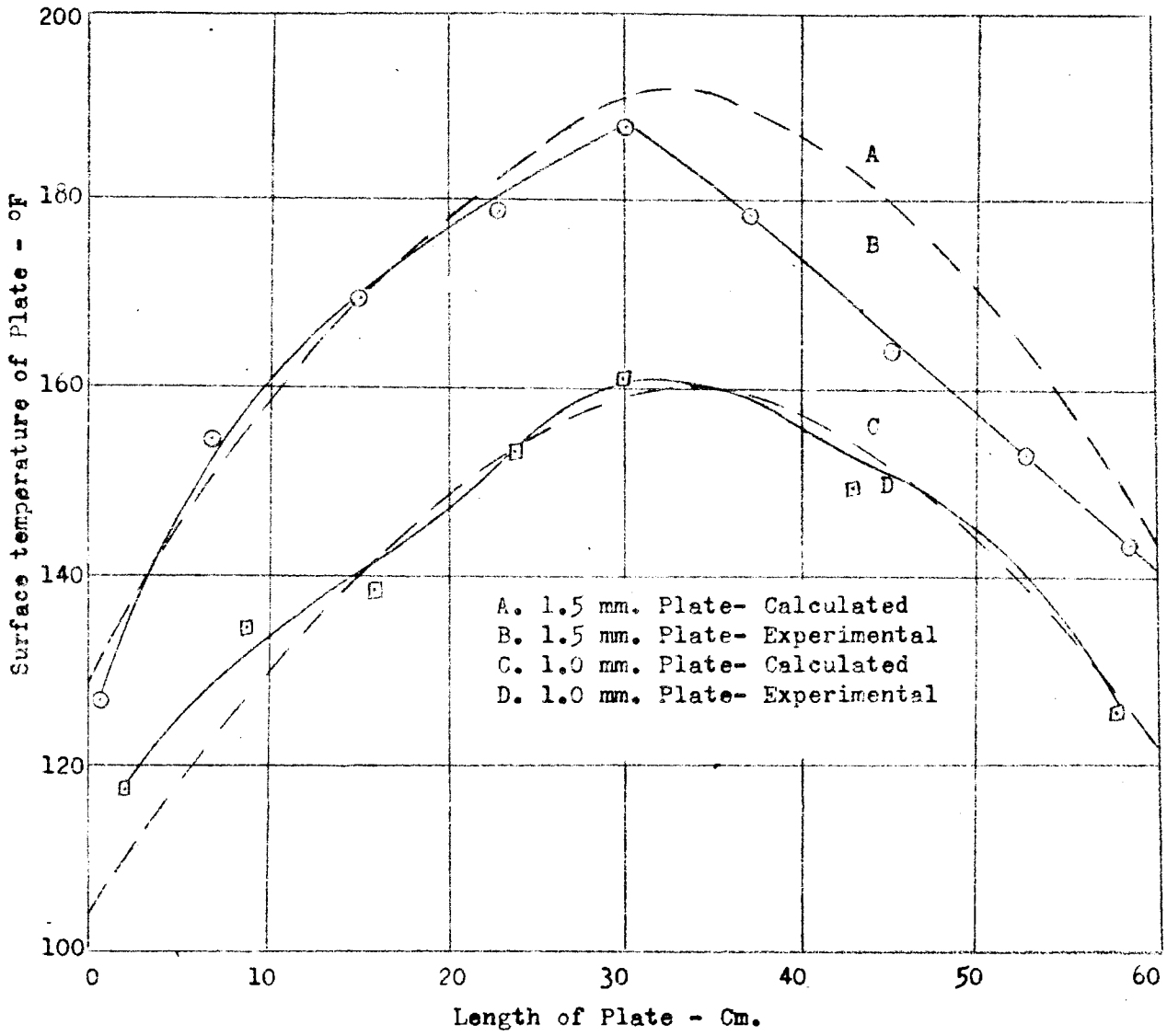

FIGURE 13 LONGITUDINAL TEMPERATURE DISTRIBUTION PRODUCED EXPERIMENTALLY ALONG THE CENTER LINE IN SINGLE PLATE ASSEMBLIES

Drawing # 5965

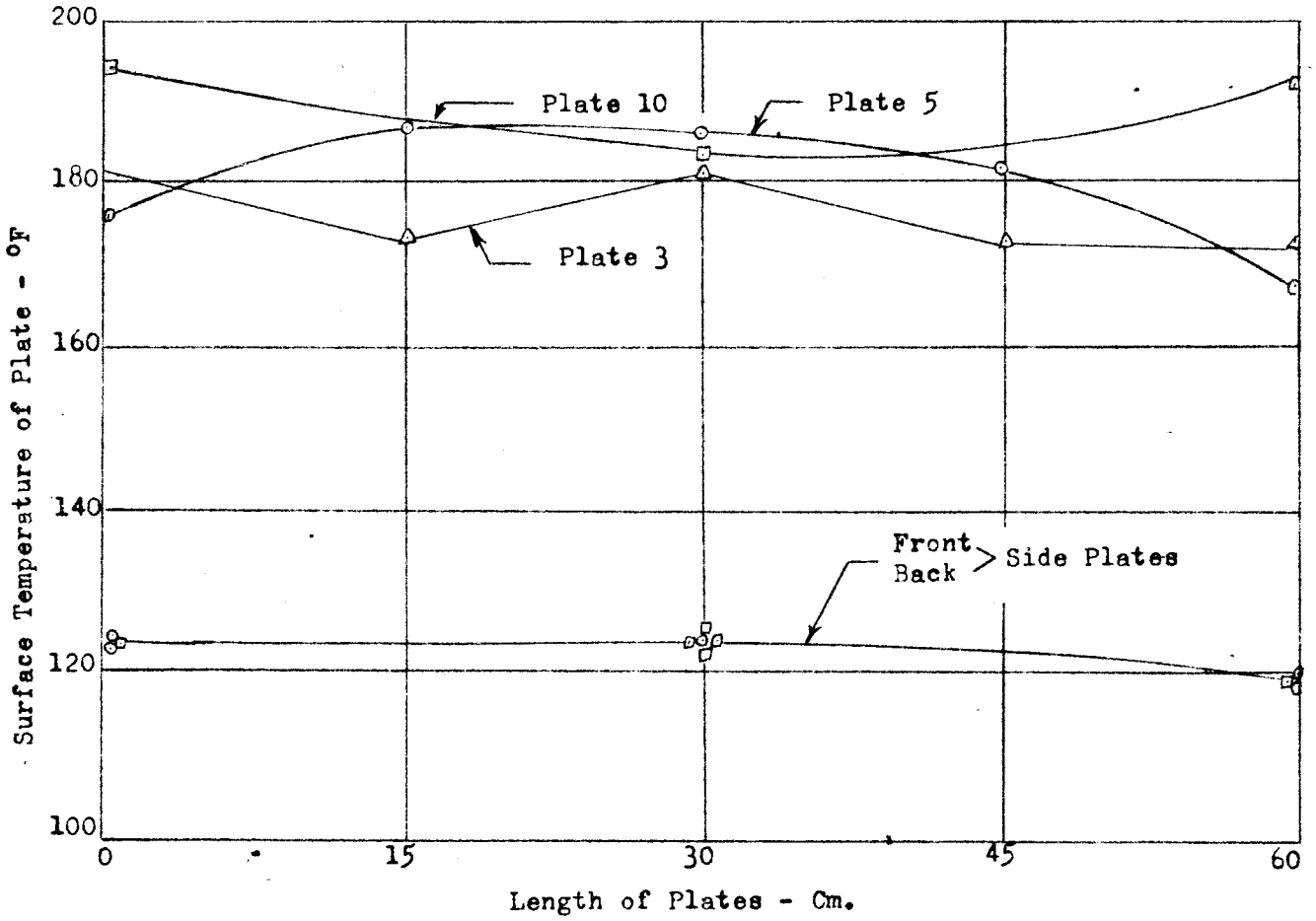

FIGURE 14 LONGITUDINAL TEMPERATURE DISTRIBUTION PRODUCED EXPERIMENTALLY IN A MULTIPLATE ASSEMBLY ALONG THE PLATE CENTER LINE

Drawing # 5966

[redacted]

Drawing # 5967

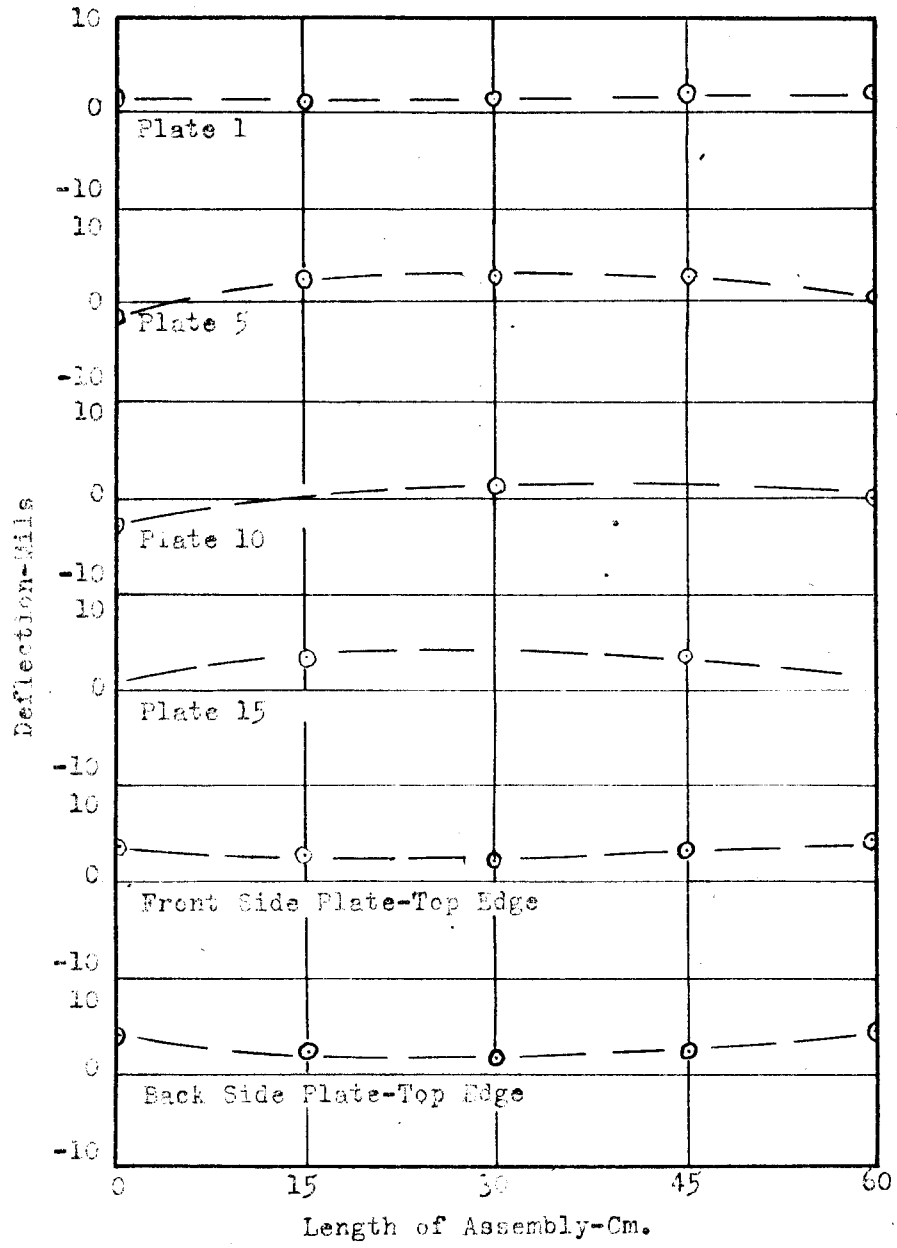

Figure 15 Summary Deflection Results From 8-Day Thermal Cycling Tests

Deflection Represents Change in Position of Assembly Plates When Heated From 60°F to Pile Operating Temperature, i.e. T Maximum-185°F-Edge ΔT-63°F

Conducted on a Multiplate Assembly Containing 18 1.5 mm. Curved Plates

[redacted]

in multiplate assemblies may be attributed to, at least, two temperature conditions. The first condition is the thermal expansion of the supporting side plates. This effect accounts for a maximum of 0.002 inches movement of the top plate and one half that amount for plate 10. The more significant bowing results from stresses which exist along the plate edges because of the sharp temperature drop.

The characteristic bowing was of the same magnitude in a single 1 mm thick plate subassembly. It is re-emphasized that both the edge effect temperature drop and the cosine distribution were produced in this assembly. See Figure 16.

A 1.5 mm plate which was approximately 20° C cooler than adjacent plates produced a constant longitudinal deflection of 0.002 inches. No appreciable bowing was observed. The amount of deflection agrees with that expected from side plate expansion. A temperature drop of not more than 15° C existed across the plate edges, thus edge stress was less by a factor of two than in the plates at a normal temperature level.

No permanent bowing or deflection was observed in multiplate assemblies containing 1.5 mm thick plates as a result of alternate heating and cooling and prolonged heating tests. Calculated stresses for the test conditions indicated that no permanent set should occur in either the 1.5 mm or 1.0 mm thick plate assemblies since the stresses were considerably below the metal yield point.

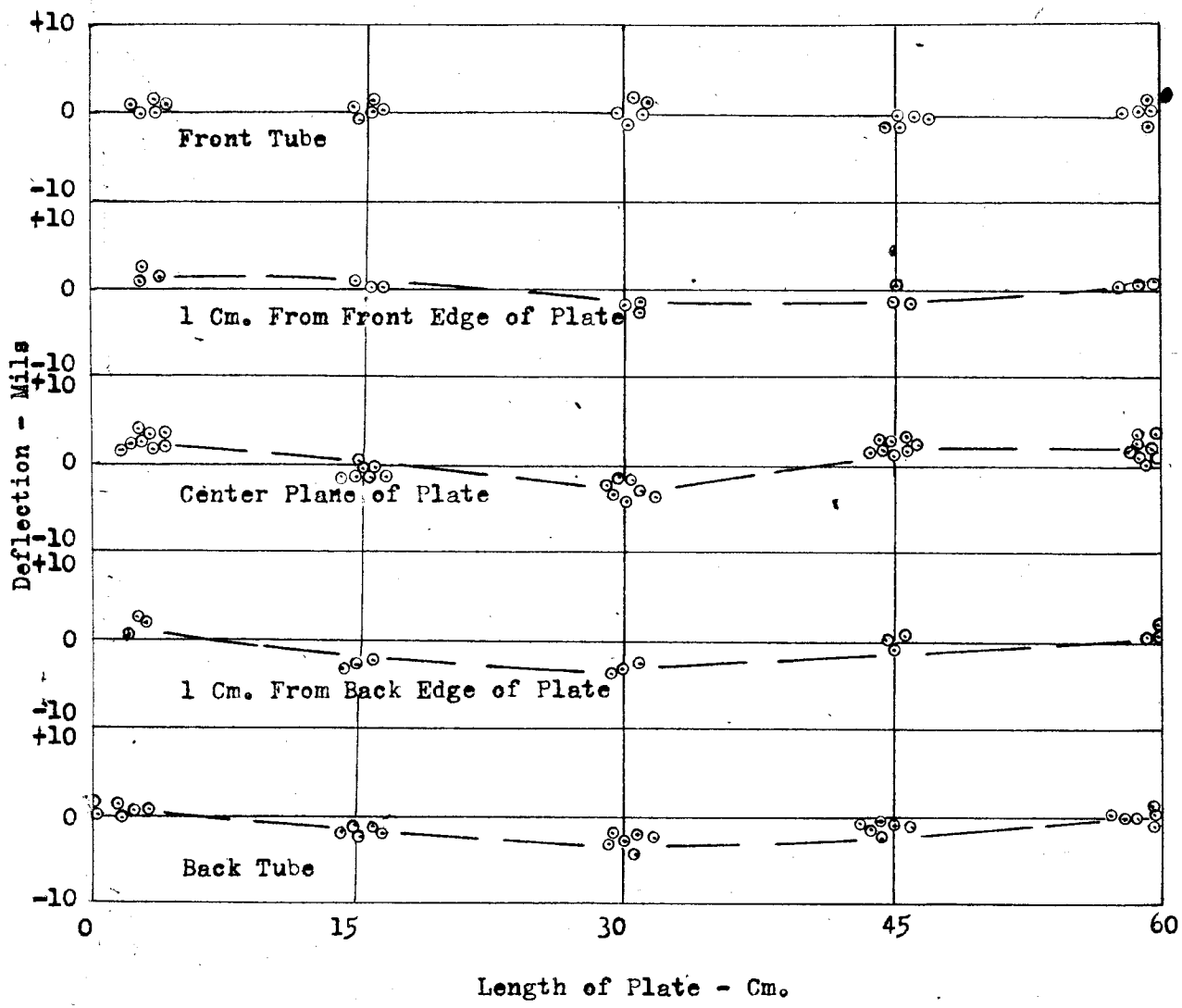

FIGURE 16 - THERMAL DEFLECTION IN A SINGLE 1 MM. FLAT PLATE ASSEMBLY
Deflection Represents the Change in Position of the Plate
When Heated From 60°F to Pile Operating Temperature.

Drawing # 5968

Test results on a single 1 mm thick plate subassembly showed no permanent set. However, a 1.5 mm thick single plate model was deformed during the first heating and cooling cycle. Investigation of the nonconforming case revealed a temperature drop which was much more severe than desired by a factor of 2. Calculated stress for this case exceeded the plate yield point. In subsequent cycles the plate returned to the new set position upon cooling. It is likely that the plate was strained sufficiently in the first cycle to produce a stress above the yield point. However, from a new position, the plate was strained less on additional heating.

Longitudinal thermal expansion was observed to be 0.020 - 0.030 inches in the 1.5 mm plate assembly. When only the edge effect temperature drop was produced the assembly expansion was 0.025 - 0.030 inches as compared to a calculated value of 0.028 inches. When the edge effect and cosine distribution were produced, the mean assembly temperature was several degrees lower with a resulting expansion of 0.020 to 0.025 inches as compared to a calculated value of 0.022 inches.

In the 1.0 mm thick single plate assembly longitudinal expansion was 0.01 inches. Calculated expansion was 0.007. Lateral expansion of assemblies containing 1.0 mm and 1.5 mm thick active plates was less than experimental accuracy of the measuring instrument of 0.002 inches.

Bowing in the single 1.5 mm thick plate subassemblies was of the order of 0.025 inches, Figures 17 and 18. The abnormally large bow was caused by

[redacted]

Drawing #5969

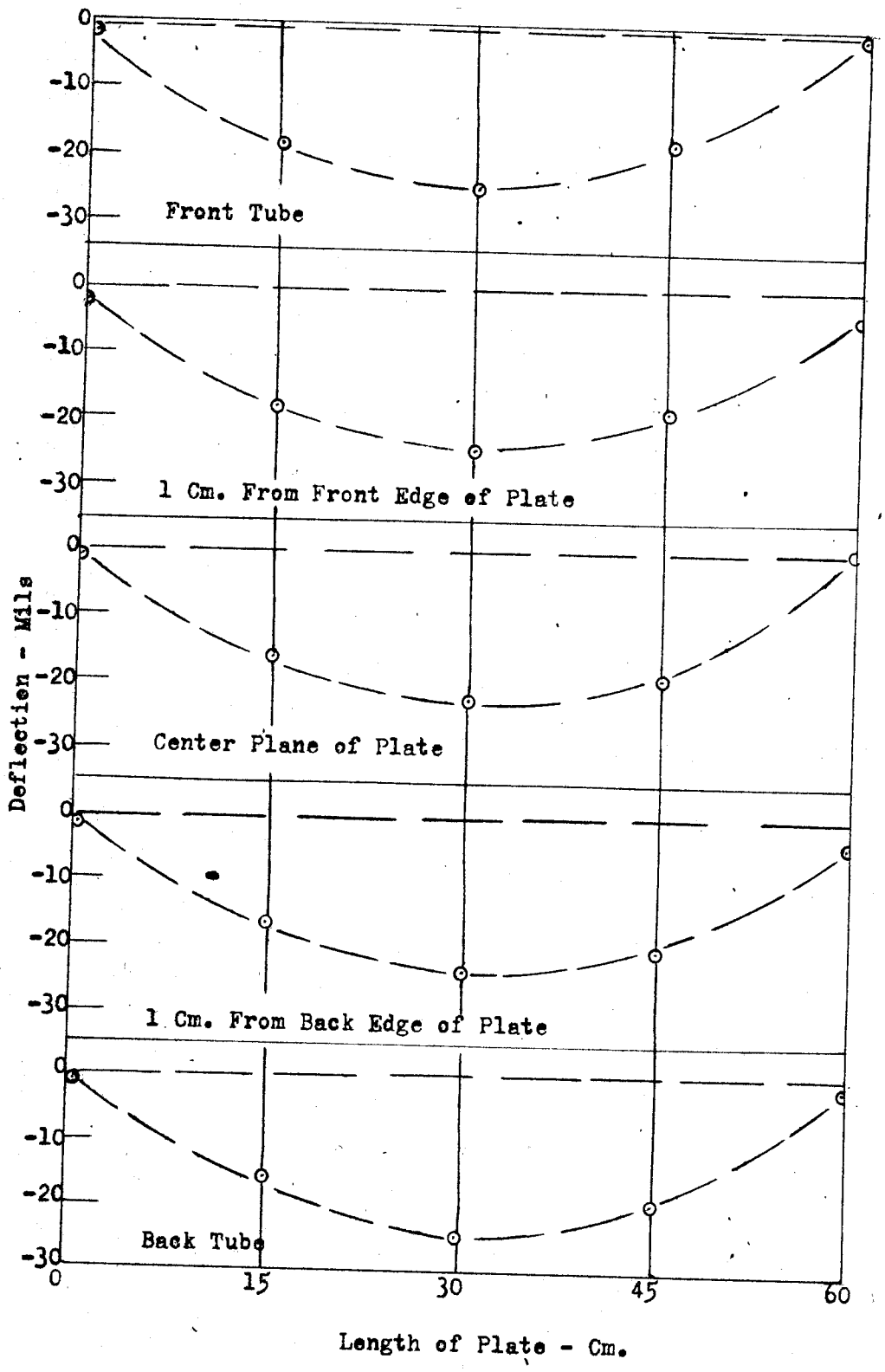

FIGURE 17 - THERMAL DEFLECTION IN A SINGLE 1.5 MM. FLAT PLATE ASSEMBLY
Deflection Represents the Change in Position of the Plate
When Heated From 60°F. to Pile Operating Temperature

[redacted]

[redacted]

Drawing # 5970

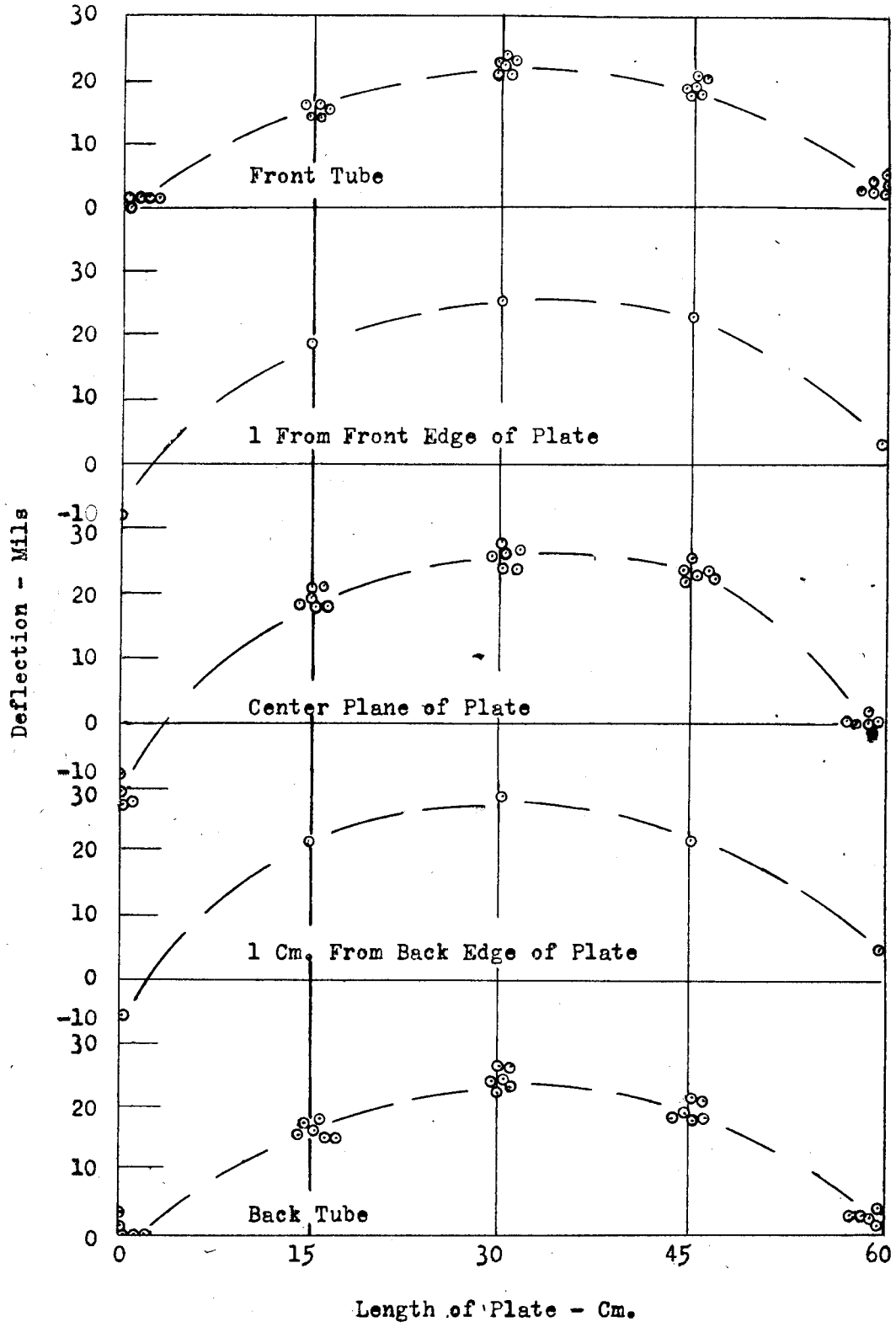

FIGURE 18 - THERMAL DEFLECTION IN A SINGLE 1.5 MM. CURVED PLATE
Deflection Represents the Change in Position of the Plate When Heated From 60°F to the Pile Operating Temperature.

[redacted]

a much too severe temperature drop across the plate edges which resulted in stresses that were high by a factor of two over the normal case. Work was dropped at this point in favor of the then available multiplate assemblies.

A last point which should be mentioned is the effect of a temperature gradient across the width of the assembly side plates. In some tests in which spray cooling was used the top edges of the plates remained 5 to 8° C cooler where water first contacted the metal surface than at the bottom edge where the water had gained heat. A bow of 0.002 inches in the direction of the cooler top edge resulted.

8.0 ESTIMATION OF ERROR

Temperature results may be considered accurate within ±2° C. Plate expansion data are accurate to ±0.002 inches. Plate deflection values are accurate to ±0.001 inches.

9.0 APPENDIX

9.1 Derivation of equation defining temperature distribution in a uranium assembly based on neutron flux pattern, G. F. Quinn, R. B. Briggs, and W. B. Allred

The power generation function over the length of an assembly is given by: $f(n) = \cos \pi x/L$

where: x = distance from center of assembly, ft.

L = distance for an angle change of π, ft.

It follows that the heat generation function will be the same.

In the assembly the active metal length 2b, is 60 cm. or 2.0 ft. Reflector requires an addition of 9 cm. to each end, L = 78 cm. or 2.5 ft. If Q is Btu/hr generated over the length, the power generated at any point along the length of active element is

2) $$dQ = A \cos \frac{\pi x}{L} dx$$

A is a constant depending on Q, and determined as follows:

$$Q = \int dQ = A \int_{-b}^{b} \cos \frac{\pi x}{L} dx$$

Integrating and simplifying

$$Q = \frac{2AL}{\pi} \left(\sin \frac{\pi b}{L}\right)$$

Solving for A

3) $$A = \frac{\pi Q}{2L \sin \frac{\pi b}{L}} \quad \text{(Btu/(hr)(ft)}$$

If W #/hr of coolant with heat capacity C and inlet temperature of T_W flows through an annulus the temperature at any distance x, T_u is given by:

$$CW\,(T_u - T_W) = A \int_{-b}^{x} \cos \frac{\pi x}{L}\, dx$$

By integrating and collecting terms the equation becomes

$$4)\quad T_u - T_W = \frac{AL}{CW\pi}\left(\sin \frac{\pi x}{L} + \sin \frac{\pi b}{L}\right)$$

If T_m is temperature of aluminum surface, the heat removal may be equated as:

$$(T_m - T_u)\, h\, p dx = A \cos \frac{\pi x}{L}\, dx$$

Where p represents the perimeter of heat transfer surface on a plane normal to the axis of the assembly.

$$5)\quad T_m - T_u = \frac{A}{hp} \cos \frac{\pi x}{L}$$

Equating 4 and 5 and solving for T_m

$$6)\quad T_m = \frac{A}{hp}\left(\cos \frac{\pi x}{L}\right) + \frac{AL}{CW\pi}\left(\sin \frac{\pi x}{L} + \sin \frac{\pi b}{L}\right) + T_W$$

9.2 Derivation of Curve for Temperature Gradient at Edge of Sandwich - G. Ascoli and R. N. Lyon

Consider the case of a fin infinitely wide in two directions from an interface. See Figure 2. The y direction is along an enriched uranium sandwich. The f direction is along the aluminum sealing strip. Assume heat is either transferred along y axis or lost at fin surfaces. Unit length is considered. Assume conductivities, K, of sandwich and sealing strip are equal.

For i $\longrightarrow$ y

Heat flow is

$$Q_y = -tK \frac{dT_y}{dy} \qquad (1a)$$

where t = fin thickness

K = thermal conductivity coefficient

T_y = temperature above water temperature

Q_y = is heat transferred per unit time in y direction

Differentiating

$$\frac{dQ_y}{dy} = -tK \frac{d^2T_y}{dy^2} \qquad (2a)$$

But by heat balance

$$\frac{dQ_y}{dy} = \sigma - 2hT_y = -(2hT_y - \sigma) \qquad (3a)$$

if σ = total heat produced per unit y

h = film coefficient

Substituting for $\frac{dQ}{dy}$ in

equation (3a) and changing sign and

substituting $\frac{1}{2h} \frac{d^2(2hT_y - \sigma)}{dy^2}$

for $\frac{d^2T_y}{dy^2}$

$$\frac{tK}{2h} \frac{d^2(2hT_y - \sigma)}{dy^2} = 2hT_y - \sigma \qquad (4a)$$

A general solution for this differential equation is

$$2hT_y - \sigma = A_y e^{\sqrt{\frac{2h}{Kt}}\, y} + B_y e^{-\sqrt{\frac{2h}{Kt}}\, x} \qquad (5a)$$

For i $\longrightarrow$ f

Heat flow is

$$Q_f = -tK \frac{dT_f}{df} \qquad (1b)$$

Q_f = heat transferred per unit time in f direction

Differentiating

$$\frac{dQ_f}{df} = -tK \frac{d^2T_f}{df^2} \qquad (2b)$$

But by heat balance

$$\frac{dQ_f}{df} = -2hT_f \qquad (3b)$$

h = film coefficient

Substituting for $\frac{dQ_f}{df}$ in equation (3b)

and substituting

$$\frac{1}{2h} \frac{d^2(2hT_f)}{df^2}$$

for $\frac{d^2T_f}{df^2}$

$$\frac{tK}{2h} \frac{d^2(2hT_f)}{df^2} = 2hT_f \qquad (4b)$$

The general solution is

$$2hT_f = A_f e^{\sqrt{\frac{2h}{Kt}}\, f} + B_f e^{-\sqrt{\frac{2h}{Kt}}\, f} \qquad (5b)$$

where A_x and B_x are constants

When y becomes large, T_y approaches the finite limit, $T_m = \frac{\sigma}{2h}$

$\therefore A_y$ must be 0

Now

$$2hT_y - \sigma = B_y e^{-\sqrt{\frac{2h}{Kt}}\, y}$$

Solving for T_y

$$T_y = \frac{B_y}{2h} e^{-\sqrt{\frac{2h}{Kt}}\, y} + \frac{\sigma}{2h} \qquad (6a)$$

When y = 0

$$2hT_y - \sigma = 2hT_i - \sigma$$

Where T_i is temperature at interface.

At the interface

$$B_y = B_f - \sigma \qquad (7a)$$

Next differentiate T_y in Eq. (6a) with respect to y

$$\frac{dT_y}{dy} = -\frac{B_y}{2h}\sqrt{\frac{2h}{Kt}}\; e^{-\sqrt{\frac{2h}{Kt}}\, y}$$

or

$$Q_y = tK\,\frac{B_y}{2h}\,\frac{2h}{Kt}\, e^{-\sqrt{\frac{2h}{Kt}}\, y} \qquad (8a)$$

At y = 0

$$Q_{yi} = tK\,\frac{B_y}{2h}\sqrt{\frac{2h}{tK}}$$

or in terms of B_f

$$Q_{yi} = \frac{B_f tK}{2h}\sqrt{\frac{2h}{Kt}} - \frac{\sigma\, tK}{2h}\sqrt{\frac{2h}{Kt}}$$

A_f and B_f are constants

When f becomes large, $T_f \longrightarrow 0$

$\therefore A_f = 0$

Now

$$2hT_f = B_f e^{-\sqrt{\frac{2h}{Kt}}\, f}$$

Solving for T_f

$$T_f = \frac{B_f}{2h} e^{-\sqrt{\frac{2h}{Kt}}\, f} \qquad (6b)$$

When f = 0

$$2hT_f = B_f = 2hT_i$$

Where T_i is temperature at interface.

Then

$$B_f = B_y + \sigma \qquad (7b)$$

Next differentiate T_f in Eq. (6b) with respect to f

$$\frac{dT_f}{df} = -\frac{B_f}{2h}\sqrt{\frac{2h}{Kt}}\; e^{-\sqrt{\frac{2h}{Kt}}\, f}$$

or

$$Q_f = tK\,\frac{B_f}{2h}\sqrt{\frac{2h}{Kt}}\; e^{-\sqrt{\frac{2h}{Kt}}\, f} \qquad (8b)$$

At f = 0

$$Q_{fi} = tK\,\frac{B_f}{2h}\sqrt{\frac{2h}{Kt}}$$

or in terms of B_y

$$Q_{fi} = -\frac{B_y tK}{2h}\sqrt{\frac{2h}{Kt}} + \frac{\sigma\, tK}{2h}\sqrt{\frac{2h}{tK}}$$

By heat balance

$$Qyi = - Qfi \qquad (9a)$$

Substituting in terms of By

$$\frac{tK}{2h}\sqrt{\frac{2h}{Kt}}\ By = -\frac{tK}{2h}\sqrt{\frac{2h}{Kt}}\ By - \frac{tK}{2h}\sqrt{\frac{2h}{Kt}}\ \sigma$$

Simplifying

$$2By = -\sigma; \quad By = -\frac{\sigma}{2} \qquad (10a)$$

Substituting value for By in eq. (6a)

$$Ty = \frac{\sigma}{2h} - \frac{\sigma}{4h}\, e^{-\sqrt{\frac{2h}{Kt}}\, y}$$

Since $Tm = \frac{\sigma}{2h}$

$$Ty = Tm - \frac{Tm}{2}\, e^{-\sqrt{\frac{2h}{Kt}}\, y}$$

$$Ti = \frac{\sigma}{4h} = \frac{Tm}{2}$$

$$Ty = Tm - Ti\, e^{-\sqrt{\frac{2h}{Kt}}\, y} \qquad (11a)$$

By heat balance

$$Qfi = - Qyi \qquad (9b)$$

Substituting in terms of Bf

$$\frac{tK}{2h}\sqrt{\frac{2h}{Kt}}\ Bf = -\frac{tK}{2h}\sqrt{\frac{2h}{Kt}}\ Bf + \frac{tK}{2h}\sqrt{\frac{2h}{Kt}}\ \sigma$$

Simplifying

$$2Bf = \sigma; \quad Bf = \frac{\sigma}{2} \qquad (10b)$$

Substituting value for Bf in Eq. (6b)

$$Tf = \frac{\sigma}{4h}\, e^{-\sqrt{\frac{2h}{Kt}}\, f}$$

Since $Tm = \frac{\sigma}{2h}$

$$Tf = \frac{Tm}{2}\, e^{-\sqrt{\frac{2h}{Kt}}\, f}$$

$$Ti = \frac{\sigma}{4h} = \frac{Tm}{2}$$

$$Tf = Ti\, e^{-\sqrt{\frac{2h}{Kt}}\, f} \qquad (11b)$$

[redacted]

Modification of case of Temperature Gradient at Edge of Sandwich Plates when the Side Walls are considered an Extension.

From the case of the fin in Appendix 9.2 the heat flowing past the interface between the sandwich and sealing edge is defined as

$$Qyi = tK \frac{By}{2h} \sqrt{\frac{2h}{tK}}$$

where t = fin thickness ft

k = coefficient of thermal Btu/hr/ft^2/ft/^{o}F conductivity

h = heat transfer coefficient at fin surfaces Btu/hr/ft^2/^{o}F

By = $2hT_i - 2hT_m$ defined from equation 6a when

y = 0 in Appendix 9.2

T_i = Surface temperature above water temperature at interface - ^{o}F

T_m = Maximum surface temperature of fin above water temperature - ^{o}F

It then can be reasonably assumed that the heat flow at the interface as shown in Figure 19 is the same as for the fin.

$$Qyi = \frac{tK}{2h} (2hT_i - 2hT_m) \sqrt{\frac{2h}{tK}}$$

$$= 0.0049 \times 124 \ (41) \sqrt{\frac{2 \times 5175}{0049 \times 124}}$$

Qyi = 3260 Btu/hr

It is next assumed that the same heat loss occurs in the 1 m.m. fin between the interface and block as would occur in the first millimeter of an extended fin as in Appendix 9.2.

$$Q_b = Qyi\left(\frac{T_b}{T_i}\right) = 3260\left(\frac{27\ ^oF}{41\ ^oF}\right) = 2150 \text{ Btu/hr.}$$

where: T_b is surface temperature above water temperature at block junction - ^{o}F

Q_b - heat flow at block junction - Btu/hr.

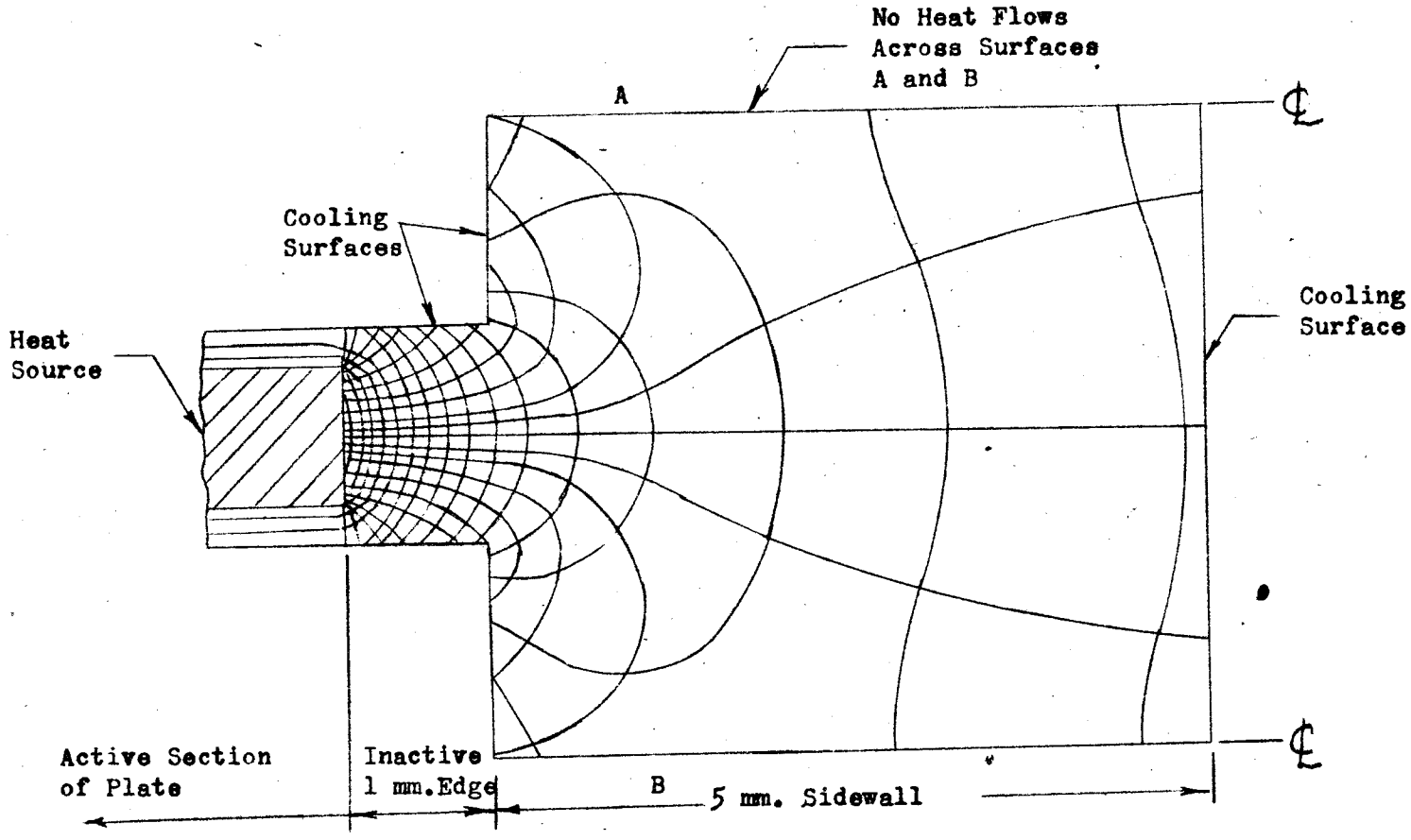

Figure 19 - GRAPHICAL SOLUTION OF HEAT FLOW THROUGH SIDE PLATE

Drawing # 5971

A graphical method as used by McAdams[11]. is now used to ascertain the flow pattern through the side wall block. The portion of the side wall shown in Figure 19 is typical for any sandwich plate. Surfaces A and B are considered as boundaries across which no heat flows.

The block is arbitrarily divided into channels which represent equal quantities of heat flow. Isotherms are then fitted to the flux channels such that the transcribed blocks are approximately square and the lines cross as perpendicular planes. The squares although unequal in size represent a constant ΔT between isotherms and a constant heat flow between flux lines. Q is then divided arithmetically according to the graph, and the system is tested to determine whether the $\Sigma \Delta T$ drop across the block and the surface h values satisfy the Q conditions of heat transfer. Calculations show that the case where 0.57 Q flows to the inside wall and 0.43Q flows to the outside wall satisfies the conditions of heat transfer.

9.3 TEMPERATURE GRADIENT THROUGH THICKNESS OF PLATE

When heat is removed at different rates from opposite faces of a reactor sheet there results a linear temperature variation across the plate superimposed on the normal symmetric distribution. The following discussion proves this statement and derives equations to determine the temperature differences. Refer to Figure 5. (1) and (2) inactive cladding, 0 alloy layer, heat source = Q $\frac{\text{Btu}}{\text{hr}}$ Conductivity = k. R = h/k (temp. base line in Figure is

11. McAdams, W. H., "Heat Transfer," McGrau Hill, 1930, Page 16.

$\frac{t_1 + t_2}{2} = 0$). The heat diffusion equations are $\frac{d^2t}{dx^2} = 0$ in (1) and (2); $\frac{d^2t}{dx^2} = \frac{-Q}{ak}$ in 0. Putting $t = \left(\frac{t_1 + t_2}{2} + \frac{t_2 - t_1}{h}\right) + t'$ we have $\frac{d^2t'}{dx^2} = 0$ in 1, 1,2; $\frac{d^2t'}{dx^2} = \frac{-Q}{ak}$ in 0 with $t'\left(-\frac{h}{2}\right) = t'\left(\frac{h}{2}\right) = 0$. From this it is obvious that t' is an even function of x, thus proving the statement. From heat balances in the two faces we have $\frac{t_2 - t_1}{R} + \frac{Q}{2} = \frac{t_1 - T_1}{R_1}$ and $\frac{t_1 - t_2}{R} + \frac{Q}{2} = \frac{(t_2 - T_2)}{R_2}$

Solving this system of equations we have

$$t_2 - t_1 = \frac{(T_2 - T_1) + \frac{Q}{2}(R_2 - R_1)}{\frac{R + R_1 + R_2}{R}}$$

$$t_1 = T_1 + \frac{T_2 - T_1 + \frac{Q}{2}(R + 2R_2)}{\frac{R + R_1 + R_2}{2}}$$

and a similar expression for t_2.

9.4 ABNORMAL CHANNEL WIDTH

If the width of a channel differs from that of its neighbors, the changed rate of flow of the coolant results in different water and plate temperatures. The following paragraphs indicate how these effects may be estimated. Refer to Figure 6. These simplifying assumptions have been made: the temperature and heat transfer coefficient in channels 2 adjacent to the abnormal channel 1 (see figure) are taken as those prevailing in a channel under normal conditions and the temperature drop across the plates is neglected. Calculations not shown here have indicated that these assumptions lead to a very small error. In the figure and in the following, absence of subscripts

indicates normal conditions and the nomenclature except as shown is that used in Section 9.3. By heat balances on the channel and plate in question we have:

$$W_1 = \frac{dT_1}{dx} = 2U_1(t_1 - T_1) \text{ and } U_1(t_1 - T_1) + U(t_1 - T) = Q \qquad (1)$$

Solving the second equation for t_1 and substituting in the first one we have after introducing the symbols of the figure and using $W \frac{dT}{dx} = Q$:

$$t_1 = \frac{\alpha T_1}{1+\alpha} + \frac{T}{1+\alpha} + \frac{Q}{(1+\alpha)U} \text{ and } \frac{d\Delta}{dx} + \frac{mU}{W}\Delta = \frac{Q_o}{W} \cos \frac{\pi x}{L_o} \qquad (2)$$

where $m = \frac{2\alpha}{B(1+\alpha)}$

L_o = length of cosine flux distribution curve

The solution of the differential equation is:

$$\Delta = Ce^{-m\frac{U}{W}N} + \frac{(m-1)}{1+m^2\left(\frac{UL_o}{\pi W}\right)^2} \frac{Q_o L_o}{\pi W} \sin \frac{\pi x}{L_o} + \frac{m(m-1)}{1+m^2\left(\frac{UL_o}{\pi W}\right)^2} \frac{Q_o}{U} \cos \frac{\pi x}{L_o} \qquad (3)$$

The constant of integration C is determined by the condition $\Delta = 0$ at the inlet, B is determined directly from the width of the channel, while α must be obtained by trial and error since it depends on the water temperature. The plate temperature may then be found from Δ by using the first of (2) and $t = T + \frac{Q}{2U}$: $t - t_1 = \frac{\alpha\Delta}{1+\alpha} + \frac{1-\alpha}{1+\alpha}\frac{Q}{2U}$

Figure 7 shows the result obtained with the design data of Section 2.0, the results shown applying to both designs.